

Self-Consistent Polarization of the Boundary in the Redistributed Charge and Dipole Scheme for Combined Quantum-Mechanical and Molecular-Mechanical Calculations

Yan Zhang,[†] Hai Lin,^{*,‡} and Donald G. Truhlar[‡]

Chemistry Department, University of Colorado at Denver and Health Sciences Center, Denver, Colorado 80217-3364, and Chemistry Department and Supercomputing Institute, University of Minnesota, Minneapolis, Minnesota 55455-0431

Received January 10, 2007

Abstract: The recently developed redistributed charge (RC) and redistributed charge and dipole (RCD) schemes are electrostatic-embedding schemes to treat a quantum-mechanical/molecular-mechanical (QM/MM) boundary that passes through covalent bonds. In the RC and RCD schemes, the QM subsystem is polarized by the MM subsystem, but the MM subsystem is not polarized by the QM one; this results in an unbalanced treatment of the electrostatic interactions. In the work reported here, we developed improved schemes, namely, the polarized-boundary RC scheme (PBRC) and the polarized-boundary RCD (PBRCD) scheme, by adding self-consistent mutual polarization of the boundary region of the MM subsystem to the previous schemes. The mutual polarizations are accounted for in the polarized-boundary calculations by adjusting the boundary-region MM point charges according to the principles of electronegativity equalization and charge conservation until the charge distributions in both the QM subsystem and the polarizable region of the MM subsystem converge. In particular, we implemented three literature parametrizations of electronegativity equalization: the original electronegativity equalization method (EEM) by Mortier and co-workers, the charge equalization (QEq) method proposed by Rappé and Goddard, and a modified version of the QEq method by Bakowies and Thiel. The PBRC and PBRCD schemes were tested by calculating proton affinities for small organic compounds and capped amino acids. As compared to full-QM calculations, the PBRC and PBRCD schemes produced more accurate proton affinities, on average, than the original RC and RCD methods; the mean unsigned error in proton affinities is reduced from about 5 kcal/mol to 3 kcal/mol with little change in geometry. The improvement is encouraging and illustrates the importance of mutual polarization of the QM and MM subsystems in treating reactions where noticeable charge transfer occurs in the QM subsystem.

I. Introduction

Combined quantum-mechanical and molecular-mechanical (QM/MM) calculations^{1–120} have become very popular in the past decade. The basic idea of QM/MM is to partition

an entire system (ES), e.g., an enzyme–substrate complex in a solvent or reagents bound to a heterogeneous catalyst into two subsystems: a localized primary system (PS) where the bond-breaking, bond-forming, and/or electron excitation processes take place and a secondary system (SS) that interacts with the PS. The PS is treated at a quantum mechanical (QM) level of theory, whereas the SS is described at the molecular mechanics (MM) level. Therefore, the PS

* Corresponding author e-mail: hai.lin@cudenver.edu.

[†] University of Colorado at Denver and Health Sciences Center.

[‡] University of Minnesota.

is also called the QM subsystem, and the SS is known as the MM subsystem. Because the precise partitioning of a system into a QM and an MM subsystem does not have a basis in experiment or quantum theory, it is somewhat arbitrary, but the concept of a partition can be justified theoretically by the observation that in many reactions the electronic structure of only a small number of atoms changes significantly. The QM/MM energy for the entire system (ES) can be formally defined as the sum of the QM energy of the PS, the MM energy of the SS, and the QM/MM interaction energy between them.

$$E(\text{QM/MM;ES}) = E(\text{QM;PS}) + E(\text{MM;SS}) + E(\text{QM/MM;PS|SS}) \quad (1)$$

In comparison with isolated QM calculations on model systems, the inclusion in eq 1 of the interactions between the PS and its surroundings (the SS) provides a more realistic description of the reactive system. For large systems, in principle, the QM/MM description combines the accuracy of a quantum mechanical description with the low computational cost of molecular mechanics, making computations for large-size reactive systems feasible. However, in order to achieve this ideal situation, the QM/MM interaction must not be oversimplified.

The interactions between the PS and the SS include valence interactions, van der Waals (VDW) interactions, and electrostatic interactions. The valence interactions require special procedures (e.g., link atoms^{3,5,11,24,40–42,50,72,76,107,111,119} or localized orbitals^{6,9,15,33,51,77,78,85,87,102,109,113}), and the van der Waals interactions are typically evaluated at the MM level. The electrostatic interactions are treated differently in various QM/MM schemes, and they are the main focus of the present article. Bakowies and Thiel¹⁶ have classified the treatments of these electrostatic interactions into two general kinds of approach. In mechanical-embedding schemes, the electrostatic interactions between the PS and SS are computed at the MM level, e.g., by Coulomb's law employing atomic charges assigned to both the PS and SS atoms, and the QM calculations for the PS are performed in the gas phase. The second and more advanced kind of treatment is called electrostatic-embedding and involves QM computations for the PS that are carried out by including in the QM Hamiltonian the operators that describe the electrostatic interaction between the nuclei and electrons of the PS and the MM partial atomic charges of the SS. In such a case, the QM/MM energy can be defined by¹⁰⁷

$$E(\text{QM/MM;ES}) = E(\text{MM;ES}) - E(\text{MM;PS}^*) + E(\text{QM;PS}^{**}) \quad (2)$$

Here the asterisk (*) denotes that the PS is embedded in the electrostatic field of the SS, and the double asterisks (**) denote such an embedding in an appropriately modified electrostatic field of the SS. (Examples of appropriate modifications are discussed below.) Usually the charge models developed for full-MM calculations are employed to represent the SS in the effective QM Hamiltonian of $E(\text{QM;PS}^{**})$. The use of the MM partial atomic charges is convenient for two reasons: First, most MM force fields,

like AMBER,¹²¹ CHARMM,¹²² and OPLS-AA,^{123–128} already contain parameters or protocols for generating the needed partial atomic point charges for calculating electrostatic interactions at the MM level. Second, many electronic-structure programs (e.g., *Gaussian03*,¹²⁹ *TURBOMOLE*,⁹² and *ORCA*¹³⁰) have the functionality of carrying out QM calculations with background point charges, and one does not need to modify the QM codes. More sophisticated representations of the SS charge density include distributed multipoles and the effective fragment potential (EFP) developed by Gordon and co-workers,¹⁹ but multipole expansions suffer from the strong dependence of the parameters on geometries,^{131–133} which limits the transferability of the parameters.¹³⁴ By including the electrostatic field due to the charge distribution of the SS into the embedded-QM calculations, the electrostatic-embedding schemes allow the PS to be polarized by the SS. The polarization perturbs the electronic structure of the PS, and it changes the energy profile of the reaction. It can even change the electronic ground state of the reagents, especially for those systems having two or more low-energy electronic states.⁸³

The polarization in the electrostatic-embedding scheme described above is unbalanced, because the PS is polarized by the SS, but the SS is not polarized by the PS. In principle, the PS and SS will polarize each other until their charge distributions are self-consistent. Schemes that allow such mutual polarization are called self-consistent mutual-polarized-embedding schemes or polarized-embedding schemes for short.¹⁶ The polarized-embedding schemes should be more accurate than electrostatic-embedding schemes, but the price that one has to pay for them is a more expensive computational cost. Complete development of the polarized-embedding QM/MM method requires a polarizable MM force field^{135–150} that has the flexibility to respond to a perturbation by an external electric field; such flexibility is not available yet in today's most popular MM force fields. Nevertheless, attempts have been made to develop polarized-embedding QM/MM schemes by combining unpolarizable MM potentials (such as AMBER,¹²¹ CHARMM,¹²² and OPLS-AA,^{123–128}) with classical polarization models.^{17,137,140,151–161} In practice these procedures are equivalent to employing polarizable force fields, but they do not assume that a generally parametrized polarizable force field is already available. The basic idea is similar to reaction field theory,^{162–164} although the response is now given by a discrete model incorporating the atomic polarizability of individual SS atoms instead of by a continuum. The classical polarization models that can be used can largely be divided into three categories: the first kind of models is based on induced dipoles (or induced multipoles),^{137,158–161} the second kind of models is based on the principle of electronegativity equalization,^{17,140,151–157} and the third is the shell model of Dick and Overhauser.¹³⁵

The first kind of polarized-embedding QM/MM scheme adds induced dipoles to the SS atomic centers^{14,16,28,114} so that the SS can respond to the electric field generated by the PS. One might wish to follow the more general theory of Stone¹⁶⁰ and assign polarizabilities of various orders (rather

than just dipole polarizabilities) to a variety of regions of the system (rather than just atomic centers). However, including only induced dipoles at atomic centers is often the most practical compromise of affordability and accuracy. Thole's empirical¹⁵⁹ treatment has been employed to model the damped behavior of short-range polarization.¹⁶ The induced dipoles are typically re-expressed as pairs of point charges in the vicinity of the SS atomic centers so as to take advantage of the ability of QM codes to carry out embedded-QM calculations with background point charges. Fitting the induced dipoles to charges on selected atomic centers is also possible.^{161,165}

The second kind of polarized-embedding QM/MM scheme allows the MM point charges in the SS to adjust in the presence of the PS^{17,27,32,154–157} according to the principle of electronegativity equalization and the principle of charge conservation; this kind of method has been labeled in a number of different ways including charge equilibration and chemical potential equalization. Since MM point charges include the contributions due to higher-order multipoles implicitly, i.e., the higher-order contributions are folded into the parameters, the adjustment of MM point charges by electronegativity equalization is a powerful way to include the response of the PS charge distribution to an external electric field and thus to account for the polarization effects. The advantage of using only point charges instead of the dipoles and higher-order multipoles is higher computational efficiency, since the computational effort is roughly proportional to the square of the number of charge sites but nine times the square of the number of dipole sites.¹⁴³ However, the polarization response of a point-charge-only model is limited in certain cases.¹⁴⁰ For example, there is no out-of-plane response for a planar molecule like benzene or water. That is, the point-charge-only model cannot represent the polarization of a benzene molecule if the external electric field is perpendicular to the molecular plane. By adopting a point-charge-only polarization model, one makes a compromise between accuracy and efficiency. For applications to large biomolecules, the errors due to the neglect of higher-order terms in the polarization treatment are often not significant, although they may be of central importance for cation- π interactions and stacking. In many cases, though they are likely to be smaller than the errors due to other approximations in the QM/MM methodology. It is also possible to improve the point-charge-only polarization model by adding a small numbers of polarizable dipoles, as has been done in the combined fluctuating charge-dipole model by Stern et al.¹⁴³

The third kind of polarized QM/MM implementation^{67,69,166} uses the ion-shell model¹³⁵ and is mainly applied in the studies of solid-state materials such as metals, metal oxides, and surface-adsorbate systems. A notable difference between crystalline materials and liquids is the periodicity of the lattices of the crystals. Usually, in QM/MM simulations of crystalline materials,^{2,20,31,43,54,64,66,67,69,73,95,166–169} the PS is treated by a cluster model embedded in a finite number of point charges (and higher-order multipoles) that mimic the infinite and periodic charge distribution of the environment (the SS). The finite number of point charges, which model

the charge-distribution of the SS, can be obtained by minimizing the difference between the electrostatic potential that is generated by the point charges and that generated by the infinite and periodic charge distribution at a set of sampling points in the active site. By doing so, one truncates the infinite and periodic system to a finite embedded cluster model, which is now much easier to handle. The polarization effects on the SS are taken into account by using the shell model,¹³⁵ which represents an ion by two charges (a positive core and a negative shell) connected by a harmonic potential. In response to the external electric field, the positions of the charges are adjusted to achieve the lowest energy.

A general conclusion that emerges from the polarizable-embedding QM/MM calculations^{10,16,27,28,32,114} is that the polarization of the SS by the PS is most significant when the PS is charged and generates large electric fields. The polarization of the SS by the reactant PS may be similar to that by the product PS so that there is some cancellation when computing relative energies (such as the energy difference between the reactants and the products), especially if the charge distribution of the PS does not change significantly during the reaction. In such a case, the effect of polarization of the SS may be less important. However, if there is significant charge transfer in the PS during a reaction, one cannot expect cancellation of errors.

The interactions between the PS and the SS are sometimes (unavoidably) complicated by making the QM/MM boundary pass through a covalent bond, leaving dangling bonds at the frontier atoms of the PS. Special care is needed to handle such a case. Treatments of QM/MM boundaries that pass through covalent bonds can be largely divided into two categories. The first category contains the so-called link-atom schemes that use H atoms^{5,11,24,41,42,72,80,82} or parametrized one-free-valence atoms^{40,50,76,111} to saturate the dangling bonds. The second category can be called the local-orbital schemes, because it contains schemes that use localized orbitals to provide a quantum mechanical description of the charge distribution near the QM/MM boundary. Two examples of the local-orbital schemes are the so-called local self-consistent field (LSCF) scheme^{6,9,15,77,113,170} and the generalized hybrid orbitals (GHO) scheme.^{33,51,78,85,87,102,103,109} The link-atom schemes are easier to implement, and thus they are widely used. The local-orbital schemes are theoretically more fundamental^{78,102} but more complicated. Extensive calculations have demonstrated that, if used carefully, both the link-atom and the local-orbital schemes can give reasonably good accuracy.

In a recent paper, we¹⁰⁷ developed two new electrostatic-embedding schemes to treat the QM/MM boundary by combining features of the local-orbital treatment with the link-atom treatment. Our schemes, which are called the redistributed charge (RC) scheme and the redistributed charge and dipole (RCD) scheme, use redistributed charges and dipoles as molecular mechanical mimics of the localized auxiliary hybrid orbitals in the GHO theory. As described in ref 107, we find it convenient to label the atoms in "tiers", i.e., the QM frontier atom as the Q1 atom, the MM boundary atom to which it is bonded as the M1 atom, the MM atoms directly connected to the M1 atom as M2 atoms, the MM

atoms directly connected to the M2 atoms as M3 atoms, and so on. In our treatment, a hydrogen link atom replaces the boundary atom and active hybrid orbital of GHO theory. This link atom, which is denoted HL, is placed on the Q1–M1 bond. The Q1–HL distance $R(\text{Q1} - \text{HL})$ depends on the Q1–M1 distance $R(\text{Q1} - \text{HL})$ by a scaling factor C_{HL} :

$$R(\text{Q1} - \text{HL}) = C_{\text{HL}} R(\text{Q1} - \text{M1}) \quad (3)$$

$$C_{\text{HL}} = R_0(\text{Q1} - \text{H})/R_0(\text{Q1} - \text{M1}) \quad (4)$$

Here $R_0(\text{Q1} - \text{H})$ and $R_0(\text{Q1} - \text{M1})$ are the MM bond distance parameters for the Q1–H and Q1–M1 stretches in the MM force field, respectively. The PS, which is now capped by the HL atoms, is called the capped PS, or CPS. Consequently, the terms $E(\text{MM};\text{PS}^*)$ and $E(\text{QM};\text{PS}^{**})$ in eq 2 are replaced by $E(\text{MM};\text{CPS}^*)$ and $E(\text{QM};\text{CPS}^{**})$, respectively, giving rise to

$$E(\text{QM}/\text{MM};\text{ES}) = E(\text{MM};\text{ES}) - E(\text{MM};\text{CPS}^*) + E(\text{QM};\text{CPS}^{**}) \quad (5)$$

In the RC scheme, one evenly distributes the MM charge of the M1 atom to the midpoints of the M1–M2 bonds. The magnitude of the bond-midpoint charges is

$$q_0^{\text{RC}} = q_{\text{M1}}/n \quad (6)$$

where n is the number of M2 atoms. In the RCD scheme, the redistributed charge q_0 and the charge on the M2 atoms (q_{M2}) are further modified in order to preserve the M1–M2 bond dipoles

$$q_0^{\text{RCD}} = 2q_0^{\text{RC}} \quad (7)$$

$$q_{\text{M2},k}^{\text{RCD}} = q_{\text{M2},k} - q_0^{\text{RC}} \quad (8)$$

where $k = 1, 2, \dots, n$. The RC and RCD schemes can be viewed as providing classical analogs to the GHO quantum descriptions of the charge distribution around the QM/MM boundary. Test calculations for geometries, proton affinities, and reaction energy profiles showed that the RC and RCD schemes provide quite good accuracy in comparison with full-QM calculations.¹⁰⁷ In particular, the mean unsigned errors (MUEs) for the proton affinities for a set of seven small organic molecules are within 3–10 kcal/mol, depending on the set of partial charges used for the embedded-QM calculations. The redistribution of the charge q_{M2} also helps in alleviating the “overpolarization” of the Q1–HL bond by q_{M2} , a problem seen in many electrostatic-embedding schemes that use link atoms to cap the PS. The overall performances of the RC and RCD schemes are roughly the same as the performance of the shifted-charge scheme¹⁷¹ (denoted Shift), which also conserves the features of the charge distribution around the QM/MM boundary, and they are significantly better than the performances of those schemes that do not conserve such features.¹⁰⁷

The RC and RCD schemes are electrostatic-embedding schemes and do not treat the polarization of the SS by

the CPS. In this study, we improve the RC and RCD schemes by including polarization of a portion of the SS by the CPS. We use the approach of electronegativity equalization in treating the MM polarization of the SS. We note that Field²⁷ had explored the same idea of electronegativity equalization under the name of fluctuating charge in his polarized-embedding QM/MM scheme. Field studied cases where the PS (solute) and the SS (solvent) are not covalently bonded: methane and formaldehyde in water. In this article, we focus on the more complicated situations where the PS and SS are covalently bonded to each other.

The new schemes introduced in this paper will be called the PBRC scheme and the PBRCD scheme, where PB indicates that they are polarized-embedding schemes that polarize (P) the boundary (B) region of the SS, as described in detail below. The theory is given in section II, where we begin with general descriptions and proceed to implementation details. Test calculations are described in section III, and the results are presented in section IV. Section V discusses the performance of the PBRC and PBRCD schemes, and a summary and conclusions are presented in section VI.

II. Theory

All equations in this section are written in atomic units.

II.A. General Description of the QM/MM Polarization Treatments. In the PBRC and PBRCD calculations, the SS charges enter the QM Hamiltonian of the CPS as one-electron terms; this accounts for the polarization of the CPS due to the SS. The polarization of the SS due to the CPS is realized by the adjustment of the SS boundary-region charges in the presence of the electric field generated by the CPS. The variation of the SS charges is determined by the principle of electronegativity equalization, which includes the constraint of charge conservation.

The procedure for incorporating self-consistent polarization is as follows: First, MM charges are assigned to the SS atoms, and the self-consistent-field (SCF) iterations of the embedded-QM calculation are performed with fixed partial atomic charges on the SS atoms. Second, the electric field generated by the CPS (nuclei and electronic wavefunctions) and the unpolarized part (if any) of the SS are computed and imposed on the polarized part of the SS, and a new set of charges is determined for the polarized part of the SS by electronegativity equalization and charge conservation. The new set of SS charges replaces the old set of SS charges, and a new embedded-QM SCF calculation is performed with the updated SS charges. Iterations continue until the variations in the charges are smaller than preset thresholds. Although this iterative algorithm is acceptable for the present test calculations, it is inefficient, and for production work the polarization of the SS should be recomputed at every step of the regular CPS self-consistent-field iterations. Implemented in this way, the increase in cost as compared to the RC and RCD calculations should be negligible.

There are two general issues to be considered here. The first consideration is that we adopt a prescription that is in the spirit of the “intramolecular-charge-transfer” treatment in the fluctuating-charge model by Berne and co-workers.¹⁴⁰

In their intramolecular-charge-transfer prescription, charge transfer was allowed within each molecule but prohibited between molecules. In our prescription, which can be called an intragroup-charge-transfer prescription, the (SS) atoms in the boundary region are treated as a group, and charge transfer is allowed within this group only. In many MM force fields like CHARMM¹²² and OPLS-AA,^{123–128} the total charge on each functional group is constrained to zero (or an integer) during the parametrization, so that charges can be easily transferred to other molecules with similar chemical groupings.¹⁴⁷ Simple examples of a functional group are the CH₂ group in an *n*-butane molecule or a whole water molecule. A group can also be constructed by selectively putting together a number of atoms that are connected to each other via covalent bonds but do not belong to the same functional group, and we will use this more general approach, as explained in the next paragraph. We note that Field²⁷ also adopted the intramolecular-charge-transfer prescription in his polarized-embedding QM/MM scheme. Field studied cases where the SS is water as solvent. Because each water molecule formed a group, the intramolecular-charge-transfer prescription and the intra-group-charge-transfer prescription would be equivalent in Field's calculations.

In the intragroup-charge-transfer prescription, a given group is in the presence of the electric field generated by the CPS and the electric fields generated by the other SS groups; those electric fields are combined into one electric field, which is referred to as the "external electric field" in this study, meaning that this combined electric field is external to the given group, which responds by adjusting its charge distribution. In the PBRC and PBRCD schemes, the only SS group that we allow to polarize is called the boundary group, since it consists of all the atoms in tiers M2 and M3, even though these atoms need not belong to the same functional group, or is called the polarizable group, since there is only one polarizable group in the PBRC and PBRCD schemes. The boundary group is the only SS group within which charge redistribution is permitted. All the other charges on the SS atoms as well as the redistributed charges q_0 at the M1–M2 midpoints retain their values, and they are put into a second group called the unpolarized group. We made such an arrangement because the polarization effect due to the bond to the CPS should be most pronounced in the QM/MM boundary region where the M2 and M3 atoms reside. The goal of the charge equalization in this study is to optimize the SS charges that appear in the QM Hamiltonian for the embedded-QM calculations rather than to fully account for the polarization of the SS at the MM level, which is a task requiring the development of polarized force fields. Although the redistributed charges q_0 are very close to the QM/MM boundary, we did not allow them to change values for two reasons: First, the redistributed charges are classical mimics of the auxiliary hybrid orbitals in the GHO theory, in which each auxiliary orbital retains its electron occupation in the QM/MM calculations.^{33,51} Second, the redistributed-charge sites are very close to the M2 atom, and we found that the electronegativity equalization calculations in which q_0 were variable gave unrealistically large values for both q_0 and q_{M2} . Therefore, we treated q_0 in the same way as we

treated the SS atoms distant from the boundary, namely by fixing their charges.

The second consideration is that the polarized SS charges are used only in the embedded-QM calculations and do not effect the MM calculations of $E(\text{MM};\text{ES})$ and $E(\text{MM};\text{CPS}^*)$ in eq 5. Although it is a common practice (and is convenient) to use MM charge parameters as partial atomic SS charges in electrostatically embedded QM calculations, we should keep in mind that these parameters are not designed for this purpose. The MM partial charges are part of an MM force field that also includes, for example, van der Waals parameters that are cross correlated with the charge parameters, and the force field is parametrized to be used as a whole for calculating MM energies, not for polarizing a quantum calculation. For the same reason, it is not appropriate to use charges from the polarized-QM calculation in the MM force field. Anyway, charges need to be consistent with the rest of the formalism and cannot be transferred between formalisms without validation.

We have implemented three literature methods that are based on the principle of electronegativity equalization, in particular the charge equalization (QEq) method employing a shielded Coulomb term (SCT) by Rappé and Goddard,¹⁵³ the modified QEq method by Bakowies and Thiel (BT),¹⁷ and the original electronegativity equalization method (EEM) of Mortier and co-workers.¹⁵¹ These methods will be abbreviated as SCT, BT, and EEM, respectively. We begin with brief descriptions of the QEq and EEM methodologies in sections II.B and II.C, respectively, and these sections also include our modifications to the original formulas by inclusion of external electric fields. Full details of the QEq and EEM methods, beyond the brief descriptions given here, can be found in the literature and will not be repeated here.

II.B. Treatments Based on the QEq Method and Its Variants. In the QEq approach of Rappé and Goddard,¹⁵³ the total electrostatic energy of a molecule of N atoms is written as the sum of the energy of all atoms in the molecule and the interatomic electrostatic energy. If we apply this to the polarizable group, we obtain

$$E(Q_1 \cdots Q_N) = \sum_A \left(E_{A0} + \chi_A^0 Q_A + \frac{1}{2} J_{AA}^0 Q_A^2 \right) + \sum_{A < B} J_{AB} Q_A Q_B \quad (9)$$

where Q_A or Q_B (A or $B = 1, 2, \dots, N$) is the charge at atomic center A or B in the polarizable SS group, E_{A0} is the energy of an isolated neutral atom A , χ_A^0 is the electronegativity of this isolated atom, J_{AA}^0 is the Coulomb repulsion integral of two electrons residing at the same isolated atom, J_{AB} is the Coulomb interaction integral between unit charges on atomic centers A and B , and the last term of eq 9 is the interatomic internal electrostatic energy of this group. The chemical potential at atomic center A is given by

$$\chi_A(Q_1 \cdots Q_N) = \partial E / \partial Q_A = \chi_A^0 + J_{AA}^0 Q_A + \sum_{B \neq A} J_{AB} Q_B \quad (10)$$

Since we have applied eq 9 to a group rather than to a whole system, we must modify it so that it includes the external electric field U_{ext} , which is the summation of the field due to the CPS ($U_{\text{A,CPS}}$) and the field due to the unpolarized group charges, the latter including the contribution by the redistributed charge q_0 at the M1–M2 midpoint

$$U_{\text{A,ext}} = U_{\text{A,CPS}} + \sum_{\text{C}} J_{\text{AC}} Q_{\text{C}} \quad (11)$$

where C denotes an SS center not in the polarized group, and J_{AC} is the Coulombic interaction integral between atoms A and C. The SS centers include the SS atoms and the M1–M2 bond midpoint. The energy of atom A in the external field is written as

$$E_{\text{A,ext}} = U_{\text{A,CPS}} Q_{\text{A}} + Q_{\text{A}} \sum_{\text{C}} J_{\text{AC}} Q_{\text{C}} \quad (12)$$

Consequently, the total energy $E(Q_1 \cdots Q_N)$ of the boundary-group atoms is given by

$$E(Q_1 \cdots Q_N) = \sum_{\text{A}} E_{\text{A}} + \sum_{\text{A} < \text{B}} E_{\text{AB}} + \sum_{\text{A}} E_{\text{A,ext}} \quad (13)$$

where E_{A} is the energy of atom A (the sum of three terms in the parentheses in eq 9), and E_{AB} is the interatomic electrostatic of interaction of atoms A and B (the last term in eq 9). The atomic chemical potential at atom A is then rewritten as

$$\chi_{\text{A}}(Q_1 \cdots Q_N) = \chi_{\text{A}}^0 + J_{\text{AA}}^0 Q_{\text{A}} + U_{\text{A,CPS}} + \sum_{\text{C}} J_{\text{AC}} Q_{\text{C}} + \sum_{\text{A} \neq \text{B}} J_{\text{AB}} Q_{\text{B}} \quad (14)$$

According to the principle of electronegativity equalization, the chemical potential should be equal at all atomic centers within the molecule. This leads to N equations

$$\bar{\chi} = \chi_1 = \cdots = \chi_N \quad (15)$$

where $\bar{\chi}$ is the common value. One additional equation comes from the principle of charge conservation, which imposes a constraint on the total charge

$$Q_{\text{tot}} = \sum_{i=1}^N Q_i \quad (16)$$

Substituting eq 14 into eq 15 and using eq 16, one obtains a total of $N + 1$ equations given in matrix form as

$$\begin{bmatrix} J_{11}^0 & J_{12} & \cdots & J_{1N} & -1 \\ J_{21} & J_{22}^0 & \cdots & J_{2N} & -1 \\ \vdots & \vdots & \cdots & \vdots & \vdots \\ J_{N1} & J_{N2} & \cdots & J_{NN}^0 & -1 \\ 1 & 1 & \cdots & 1 & 0 \end{bmatrix} \begin{bmatrix} Q_1 \\ Q_2 \\ \vdots \\ Q_N \\ \bar{\chi} \end{bmatrix} = \begin{bmatrix} -\chi_1^0 - U_{1,\text{CPS}} - \sum_{\text{C}} J_{1\text{C}} Q_{\text{C}} \\ -\chi_2^0 - U_{2,\text{CPS}} - \sum_{\text{C}} J_{2\text{C}} Q_{\text{C}} \\ \vdots \\ -\chi_N^0 - U_{N,\text{CPS}} - \sum_{\text{C}} J_{N\text{C}} Q_{\text{C}} \\ Q_{\text{tot}} \end{bmatrix} \quad (17)$$

The QEq charges in the presence of an external field are obtained by solving eq 17.

The Coulomb interactions are evaluated approximately by using an empirical function. One function tested by Rappé and Goddard¹⁵³ is

$$J_{\text{AB}} = \frac{1}{\epsilon R_{\text{AB}}} \quad (18)$$

where ϵ is the dielectric constant taken to be 2, and R_{AB} is the distance between atoms A and B. Although eq 18 does not give a correct description of J_{AB} when $R \rightarrow 0$, it was shown that with $\epsilon = 2$, eq 18 produced reasonable charges for a set of molecules at their equilibrium geometries.¹⁵³ It is interesting to see whether such an empirical treatment can produce reasonable charges in the present study. For this reason, we make use of eq 18 and denote the corresponding calculations as SCT. The SCT results should be interpreted with care by keeping in mind that eq 18 is approximate and is not valid if the atoms are close to each other.

Bakowies and Thiel¹⁷ proposed a modified QEq method, where the Klopman–Ohno function^{172,173} is employed to compute the Coulomb interactions because it is more realistic than eq 18 for small R_{AB} . Their formula is

$$J_{\text{AB}} = \frac{1}{\sqrt{R_{\text{AB}}^2 + \left(\frac{1}{2J_{\text{AA}}^0} + \frac{1}{2J_{\text{BB}}^0} \right)^2}} \quad (19)$$

Employing eq 19, Bakowies and Thiel¹⁷ optimized a set of parameters for the elements H, C, N, and O for the QM/MM calculations where the QM methods are AM1¹⁷⁴ and MNDO¹⁷⁵ and the force field is MM3.^{176–178} In this article, computations employing eq 19 and the set of parameters optimized by Bakowies and Thiel are denoted BT.

II.C. Treatments Based on the EEM Model. The EEM model is also based on the principle of electronegativity equalization.¹⁵² In the EEM model, the atomic electronegativity in a molecule can be written as

$$\chi_{\text{A}} = \chi_{\text{A}}^* + 2\eta_{\text{A}}^* Q_{\text{A}} + \sum_{\text{B} \neq \text{A}} \frac{Q_{\text{B}}}{R_{\text{AB}}} \quad (20)$$

where Q_A and Q_B are charges on atoms A and B, respectively, and χ_A^* and η_A^* are defined by

$$\chi_A^* = \chi_A^0 + \Delta\chi \quad (21)$$

$$\eta_A^* = \eta_A^0 + \Delta\eta \quad (22)$$

Here, χ_A^0 and η_A^0 are the electronegativity and hardness of the isolated atom, respectively, and $\Delta\chi$ and $\Delta\eta$ are correction terms due to the fact that an atom is now in a molecule instead of being isolated, thus changing its size and shape.

Again, just as for the QEq method, we modified the original EEM equations so that they apply to a group in the presence of an external electric field U_{ext} . In this work, the external field at atomic center A in the boundary group is the summation of the field due to the CPS ($U_{A,\text{CPS}}$) and the field due to the unpolarized-group charges

$$U_{A,\text{ext}} = U_{A,\text{CPS}} + \sum_C \frac{Q_C}{R_{AC}} \quad (23)$$

where C denotes a center in the unpolarized SS group, and R_{AC} is the distance between atoms A and C. In the presence of the external field, the total energy of the boundary-group atoms can be written as

$$E = \sum_A (E_A^{\text{atm}} + E_A^{\text{int}} + E_{A,\text{ext}}) \quad (24)$$

where E_A^{atm} is the energy of atom A in the absence of external electric field, E_A^{int} is the interatomic interactions attributed to atom A, and $E_{A,\text{ext}}$ is the potential energy of atom A due to the external field. The electronegativity of atom A in the presence of the external potential is thus given by

$$\chi_A = \chi_A^* + U_{A,\text{CPS}} + \sum_C \frac{Q_C}{R_{AC}} + 2\eta_A^* Q_A + \sum_{B \neq A} \frac{Q_B}{R_{AB}} \quad (25)$$

In comparison with the expression in original EEM model (eq 20), here one has two additional terms accounting for the external field.

Upon substituting eq 25 in eqs 15 and 16, one obtains a set of $N + 1$ coupled equations. The equations are solved for the electronegativity $\bar{\chi}$ and the atomic charges. Bultinck et al. had listed in Table 1 of ref 154 several sets of EEM parameters, and we found that the set of parameters developed by Mortier and co-workers showed the best agreements between the EEM- and QM-calculated dipole moments for small organic molecules in our test calculations. Thus, we adopt in the present study the EEM parameters by Mortier and co-workers, and the corresponding QM/MM calculations are denoted EEM.

III. Computations

The new polarized QM/MM schemes, PBRC and the PBRCD, were tested by calculating geometries and proton affinities for seven small organic molecules and four capped amino acids, one of which is protonated in two different places. The proton affinity is defined as the energy difference

between a chemical species ($X^- + H^+$ or $X + H^+$) and its protonated form (XH or XH^+), each at its optimized geometry. The proton affinity is a challenging test for the QM/MM methodology, because the protonation causes significant changes in the charge distribution of the PS and proton affinities are very sensitive to the treatment of electrostatic interactions between the PS and SS. This is especially the case if the protonation site is very close to the QM/MM boundary (as it is in our test cases) and if significantly polar SS functional groups are nearby.

The small organic molecules in the test suite are $\text{CH}_3\text{--CH}_2\text{OH}$, $\text{CH}_3\text{--CH}_2\text{SH}$, $\text{CH}_3\text{--CH}_2\text{NH}_3^+$, $\text{CH}_3\text{--CH}_2\text{COOH}$, $\text{CF}_3\text{--CH}_2\text{OH}$, $\text{CH}_2\text{OH--CH}_2\text{OH}$, and $\text{CH}_2\text{OH--CH}_2\text{SH}$, where only the protonated form is listed, and the dash indicates the boundary between the SS on the left and the PS on the right. These molecules have been employed in the recent study¹⁰⁷ of the original RC and RCD schemes. The capped amino acids in the test suite are histidine, glutamic acid, lysine, and tyrosine, for which the N-terminals are capped by an acetyl (Ace) group and the C-terminals are capped by an N-methylamide (NMe) group. Figure 1a–1f shows the models of histidine (Ace-His⁺-NMe), histidine deprotonated at the δ position (Ace-His $^\delta$ -NMe), histidine deprotonated at the ϵ position (Ace-His $^\epsilon$ -NMe), glutamine acid (Ace-Glu-NMe), lysine (Ace-Lys⁺-NMe), and tyrosine (Ace-Tyr-NMe). The side chains are treated at the QM level, while the backbones are described by an MM force field.

For the present study, the Gaussian03¹²⁹ program is employed for QM calculations, TINKER¹⁷⁹ is used for MM calculations, and QMMM¹⁸⁰ is utilized for QM/MM calculations. In both the PBRC and PBRCD computations, treatments based on the QEq (including the SCT and BT treatments) and EEM schemes were tested. For comparison, we also carried out calculations employing the electrostatic-embedding RC and RCD schemes, where no polarization of the SS is allowed. Full-QM calculations were performed and were used as benchmarks for assessment of the QM/MM methods.

The QM level for the examples in this article is Hartree–Fock theory¹⁸¹ with the MIDI¹⁸² basis set, which was used in our previous paper¹⁰⁷ on the RC and RCD schemes. The OPLS-AA force field^{123–128} implemented in TINKER¹⁷⁹ was employed for the MM descriptions. For some molecules, several force field parameters were missing, and we solved the problem by using parameters for similar atom types; the parameters are given in the Supporting Information. Although the protonated and deprotonated species have different sets of atom types, we used only one set of MM parameters throughout the calculations, in particular the set of parameters for the species that has one more atom. As discussed previously,¹⁰⁷ such a selection of MM parameters is not perfect, but is the only straightforward option for reaction path calculations. Thus we are testing the methods under the conditions that would be used in actual applications to chemical reactions.

A question that arises is how the accuracy would change if we used more popular methods of electronic structure theory. To explore this issue, we carried out additional calculations with the B3LYP and MP2 levels of theory and

Table 1. Atomic Charges Derived from the Full-QM and QM/MM Calculations for the Ace-His⁺-NMe System^a

atom	QM	RC	PBRC			RCD	PBRCD		
			SCT ^b	BT ^c	EEM		SCT ^b	BT ^c	EEM
PS									
C13	−0.376	−0.514	−0.544	−0.570	−0.541	−0.475	−0.512	−0.564	−0.505
C14	0.162	0.284	0.314	0.327	0.306	0.277	0.309	0.325	0.300
N15	−0.130	−0.269	−0.288	−0.279	−0.274	−0.267	−0.286	−0.277	−0.272
C16	−0.207	−0.281	−0.277	−0.303	−0.288	−0.277	−0.275	−0.298	−0.287
C17	0.074	0.075	0.104	0.076	0.080	0.076	0.104	0.078	0.081
N18	−0.241	−0.155	−0.187	−0.159	−0.169	−0.154	−0.185	−0.159	−0.166
H19	0.168	0.186	0.179	0.179	0.181	0.186	0.180	0.190	0.182
H20	0.151	0.226	0.219	0.229	0.215	0.224	0.218	0.236	0.212
H21	0.321	0.451	0.462	0.452	0.454	0.453	0.464	0.454	0.455
H22	0.250	0.268	0.261	0.272	0.265	0.269	0.262	0.272	0.266
H23	0.229	0.237	0.227	0.234	0.234	0.238	0.228	0.234	0.235
H24	0.385	0.369	0.372	0.370	0.371	0.369	0.373	0.370	0.371
SS									
N7	−0.582	−0.500	−0.409	−0.937	−0.444	−0.547	−0.451	−0.967	−0.482
C9	0.664	0.500	0.217	0.663	0.184	0.453	0.167	0.615	0.117
H12	0.047	0.060	−0.009	0.006	0.003	0.013	−0.057	−0.031	−0.049
C2	0.762	0.500	0.361	0.702	0.451	0.500	0.359	0.689	0.450
H11	0.303	0.300	0.283	0.526	0.231	0.300	0.285	0.521	0.232
O10	−0.515	−0.500	−0.290	−0.441	−0.172	−0.500	−0.289	−0.442	−0.162
N25	−0.535	−0.500	−0.294	−0.660	−0.393	−0.500	−0.293	−0.665	−0.387
redistributed charge (q_0)	n/a	0.047	0.047	0.047	0.047	0.093	0.093	0.093	0.093
link atom (HL)	n/a	0.122	0.157	0.172	0.165	0.082	0.120	0.139	0.129

^a The side chain is the PS, and the backbone is the SS (see also Figure 1). The QM level is HF/MIDI!, and the MM force field is OPLS-AA. The iterative procedure for polarization was initiated by using the OPLS-AA charges for the embedded-QM calculations. ^b QEq model with SCT of Rappé and Goddard. ^c QEq model of Bakowies and Thiel.

the 6-31+G* basis set,^{183–186} where the B3LYP denotes the Becke 3-parameter Lee–Yang–Parr density functional method,^{187,188} and MP2 denotes Møller–Plesset second-order perturbation theory.¹⁸⁹

In the self-consistent polarization treatment, the M2 and M3 atoms in the SS constitute the boundary group, whereas the other SS atoms and the redistributed charge q_0 at the M1–M2 bond midpoint constitute the unpolarized SS group. The iterative procedure was initiated by assigning MM partial charges to the SS atoms; these may be called the initial or unpolarized charges. These unpolarized charges remain constant through the calculation for the unpolarized SS group but are just initial charges for the polarized boundary group. It is of interest to see the sensitivity of the calculations to the initial SS charges. Therefore we tried two choices for the unpolarized charges in the cases of small organic molecules, where, in addition to OPLS-AA charges, we also used charges obtained by fitting the electrostatic potential (ESP) using the Merz–Kollman algorithm;^{190,191} those ESP charges had been computed in our previous study of the RC and RCD schemes.¹⁰⁷ In that study, we found that the ESP charges worked the best among several charge models examined for electrostatically embedded QM/MM calculations of the protonation of small organic molecules in the gas phase. For the capped amino acids, we only employed the OPLS-AA charges as partial atomic charges on the SS atoms in the embedded-QM calculations in the present paper. We note that the ESP charges can be problematic for large molecules due to the large uncertainty of the charges on buried atoms derived from the fitting procedure to electro-

static potentials. Nevertheless, when they can be computed stably, the ESP charges are worthy of consideration.

The convergence thresholds of the self-consistent polarization calculations were set to 0.005 e for the maximum change and 0.002 e for the root-mean-square change in the QEq and EEM charges for the SS atoms.

Geometry optimization for large molecules is generally difficult because of multiple local minima. When comparing QM/MM and full-QM calculations, we wanted to make the comparisons for a given molecule such that the QM and QM/MM calculations have the same conformations. To accomplish this we followed a standard procedure so that the optimized geometries resemble each other in a systematic way. In particular, for a given molecule, we began by optimizing the geometry for the protonated species (XH or XH⁺) at the full-QM level; this served as a starting point both for the full-QM geometry optimization for the deprotonated species (X⁻ or X) and for the QM/MM geometry optimization for the protonated geometry. Finally, starting from the optimized QM/MM protonated geometry, we optimized the QM/MM deprotonated geometry. Visualization of the superimposed geometries ensured that the full-QM and QM/MM conformations are approximately similar to each other. For the capped amino acids, we also made comparisons of single-point energies at fixed geometries, as discussed below.

IV. Results

Figure 2 illustrates the convergence of the embedded-CPS energy in a PBRC single-point energy calculation using the

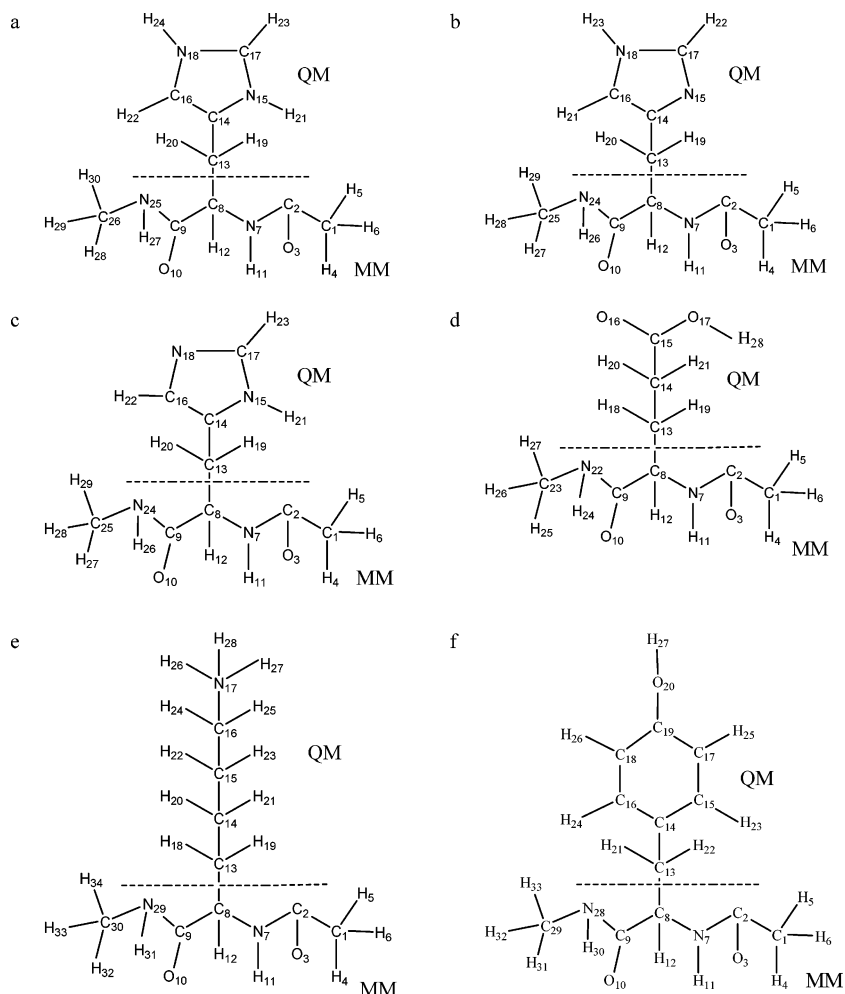


Figure 1. The capped amino acids in the test suite: (a) Ace-His⁺-NMe, (b) Ace-His^δ-NMe, (c) Ace-His^ε-NMe, (d) Ace-Glu-NMe, (e) Ace-Lys⁺-NMe, and (f) Ace-Tyr-NMe.

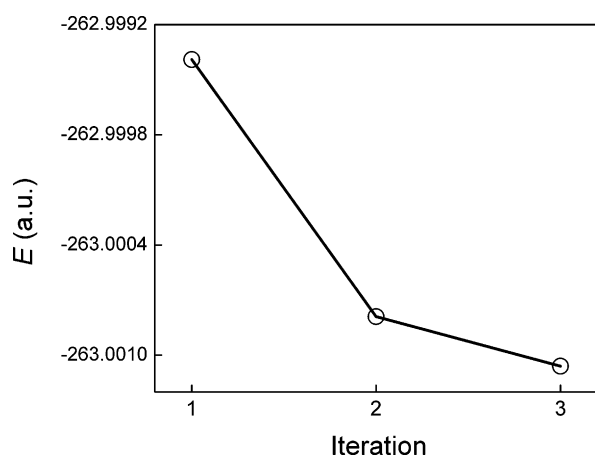


Figure 2. The convergence of the embedded-QM energy for the CPS in the Ace-His⁺-NMe system in the PBRC calculation employing the SCT scheme.

SCT parametrization for the Ace-His⁺-NMe system. The embedded-CPS energy formally includes the QM energy of the CPS, Coulombic interaction energy of the SS charges, and electrostatic interaction energy between the CPS and the SS charges. Figures 3 and 4 display for the same calculation the convergence of the ESP charges for the PS atoms and the convergence of the SCT charges for the SS atoms,

respectively. Only the heavy atoms whose charges changed by more than 0.001 e are shown in Figures 3 and 4.

In Table 1, we compare the atomic charges of Ace-His⁺-NMe derived from the full-QM and QM/MM computations; the geometries were optimized at the given levels of theory. In the case of full-QM calculation, we list ESP charges. For QM/MM calculations, we give the ESP charges for the CPS atoms including the hydrogen link atom, we give OPLS-AA charges for the SS atoms when the RC and RCD methods are used, and we give electronegativity-equalized or charge-equilibrated charges for the polarized SS atoms when the PBRC and PBRCD schemes are used (the unpolarized SS atoms of the PBRC and PBRCD methods are not shown in Table 1). The redistributed charge q_0 was fixed to $q_{M1}/3$ in the RC and PBRC calculations and to $2q_{M1}/3$ in the RCD and PBRCD calculations, where q_{M1} is the OPLS-AA charge on the M1 atom in the SS.

The proton affinities of the seven small organic molecules are listed in Table 2, where results are shown both for calculations using the OPLS-AA charges to initiate the self-consistent polarization procedure and for those using ESP charges for initialization. Table 3 tabulates the QM/MM optimized Q1–M1 bond distances for both the neutral and charged species involved in the calculations of Table 2. The QM/MM geometries and energetics are compared with full-

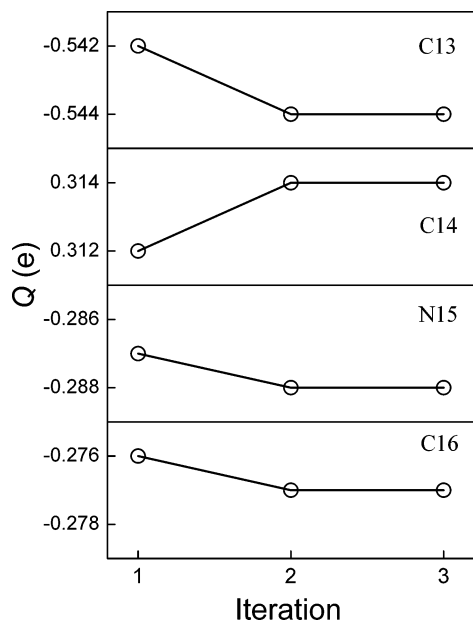


Figure 3. The convergence of the ESP charges for the CPS heavy atoms in the Ace-His⁺-NMe system in the PBRC calculation employing the SCT scheme. Two atoms C17 and N18, which are distant from the QM/MM boundary, underwent negligible (<0.001 e) changes of the charges over the iterations and are therefore not shown.

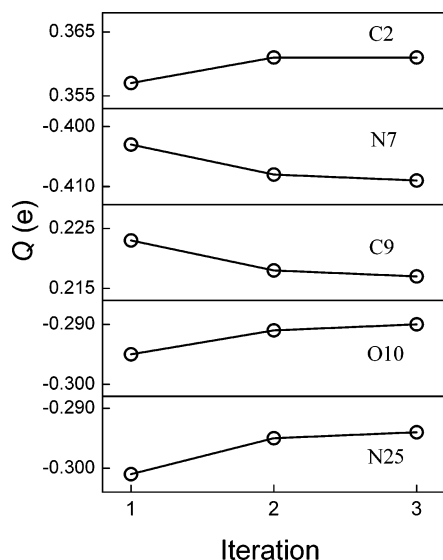


Figure 4. The convergence of the SCT charges for the SS heavy atoms in the Ace-His⁺-NMe system in the PBRC calculation employing the SCT scheme.

QM calculations, and mean unsigned errors (MUEs) and mean signed errors (MSEs) were computed in order to give an assessment of the performance for the QM/MM treatments; in particular, the MUE and MSE were calculated for each QM/MM treatment by averaging the differences between the full-QM and the QM/MM results over all involved molecules.

Because parameters are not available for the fluorine atom in the BT and the EEM parameter sets, the CF₃CH₂OH molecule was excluded from the BT and EEM calculations as well as from their MUE and MSE evaluations. Consequently, to make the comparison on the same grounds, we

computed for each of the other QM/MM treatments two sets of MUE (and MSE), one of which includes CF₃CH₂OH and the other does not. The results including CF₃CH₂OH are especially interesting in that they can be compared to our previous paper.¹⁰⁷

The proton affinities for the capped amino acids are presented in Table 4. In addition to the PBRC and PBRCd schemes where the M2 and M3 charges in the SS are polarized, we also examined (for the SCT parametrization only) a more general scheme where all SS atoms were put into a single polarizable group. Table 5 displays the QM/MM optimized Q1–M1 bond distances of the molecules involved in the calculations involved in Table 4. The MUE and MSE were computed for each QM/MM treatment by averaging over all capped amino acids and using the full-QM results as the standard reference data.

To help in examining the influence of geometry on the proton affinities of the capped amino acids, we computed the QM/MM proton affinities using the same geometries, namely, the optimized full-QM geometries, for all QM/MM schemes. These are given in Table 6, and they may be denoted as QM/MM//full-QM proton affinities, where A/B means a single-point energy calculation at the A level using a geometry optimized at the B level.

Finally, overall mean unsigned errors for proton affinities are computed in Table 7 by averaging over the results for organic molecules and capped amino acids.

V. Discussion

The discussion will focus on the calculations with QM = HF/MIDI! level of theory except for section V.E, where additional calculations with two QM levels (B3LYP/6-31+G* and MP2/6-31+G*) of theory are analyzed, and for section V.F, where an overall assessment of the new boundary treatment for all three QM levels are given.

V.A. Convergence of the Self-Consistent Polarization Procedure. There are two kinds of convergence one might consider. The first is convergence with respect to allowing more and more atoms to be polarized; the second is convergence of the self-consistent iterations for a given number of polarized atoms. The first type of convergence, however, is not one of the goals of the present paper, and the results in Table 4 show that, in practice, poor results were produced for proton affinities when all SS atoms were put into a polarizable group and were permitted to vary their charges in the self-consistent polarization procedure. Most currently available molecular mechanics force fields are parametrized to give the correct results in the absence of explicit polarization. To polarize the entire MM system would therefore require a new parametrization. However, the MM force fields were parametrized for use in a fully MM calculation, and the QM/MM boundary can introduce inconsistent electrostatic interactions that can lead to unstable or unphysical polarization. Our polarized boundary treatment is primarily directed to eliminating this problem, and so the goal is to parametrize the region that is most likely to suffer from this inconsistency (and thereby alleviate it) rather than the regions that are most polarizable. Therefore the rest of

Table 2. Proton Affinities (kcal/mol) for Small Organic Molecules^a

molecule (SS–PS)	QM ^b	initial charge	RC ^b	PBRC				PBRCD		
				SCT ^c	BT ^d	EEM	RCD ^b	SCT ^c	BT ^d	EEM
CH ₃ –CH ₂ OH	416.8	OPLS-AA	427.2	426.8	426.6	427.0	431.5	431.1	430.9	431.3
		ESP	423.9	423.6	423.4	423.8	425.4	425.0	424.8	425.2
CH ₃ –CH ₂ SH	381.5	OPLS-AA	386.7	385.9	385.5	386.4	389.5	388.6	388.2	389.1
		ESP	384.7	383.9	383.6	384.3	395.6	384.8	384.4	385.2
CH ₃ –CH ₂ NH ₃ ⁺	232.8	OPLS-AA	233.3	233.7	234.0	233.5	236.5	236.9	237.1	236.6
		ESP	231.0	231.4	231.7	231.2	232.0	232.4	232.7	232.2
CH ₃ –CH ₂ COOH	375.3	OPLS-AA	379.9	379.2	378.9	379.6	382.2	381.6	381.2	381.9
		ESP	378.1	377.5	377.2	377.9	378.9	378.3	378.0	378.6
CF ₃ –CH ₂ OH	396.8	OPLS-AA	415.5	415.3	n/a	n/a	398.7	398.4	n/a	n/a
		ESP	408.8	408.5	n/a	n/a	395.4	395.2	n/a	n/a
CH ₃ OH–CH ₂ OH	413.2	OPLS-AA	424.2	415.8	416.6	418.3	420.0	411.4	411.6	414.2
		ESP	422.0	413.6	414.1	416.2	415.3	406.6	406.1	409.7
CH ₂ OH–CH ₂ SH	376.5	OPLS-AA	383.4	378.1	379.0	380.2	380.8	375.5	375.9	377.8
		ESP	382.4	376.8	377.4	379.0	378.3	372.7	372.6	375.1
MUE (seven) ^e		OPLS-AA	6.4/8.2	3.9/6.0	4.1	4.8	7.4/6.6	5.8/5.2	5.5	5.8
		ESP	4.9/5.9	2.3/3.6	2.3	3.3	5.1/4.6	4.2/3.8	4.1	3.5
MSE (seven) ^f		OPLS-AA	6.4/8.2	3.9/6.0	4.1	4.8	7.4/6.6	4.8/4.4	4.8	5.8
		ESP	4.3/5.4	1.8/3.2	1.9	2.7	4.9/4.0	0.6/0.3	0.4	1.7

^a The QM level is HF/MIDI!, and the MM force field is OPLS-AA. The iterative procedure for polarization was initiated by using the OPLS-AA or ESP charges for the embedded-QM calculations. ^b Reference 107. The mean errors in ref 107 differ slightly from those in this paper because they were computed from unrounded data. In this paper, all mean errors were computed from data rounded to the nearest 0.1 kcal/mol. ^c QEq model with SCT of Rappé and Goddard. ^d QEq model of Bakowies and Thiel. ^e Mean unsigned error excluding/including CF₃–CH₂OH. ^f Mean signed error excluding/including CF₃–CH₂OH.

this subsection is devoted to the other convergence issue, namely convergence of the iterative steps.

Although, as pointed out above, the polarized boundary step should be included in each QM SCF step for efficiency, the present algorithm is well suited for studying convergence. For the calculations in the present work, we found rapid convergence of the self-consistent polarization iterations; typically, the convergence was achieved within three sets of iterations. This is illustrated here for the Ace-His⁺-NMe system as an example. The Ace-His⁺-NMe system was selected for demonstration because the charged CPS can have strong polarization effects on the SS and because the electron delocalization over the imidazole ring in the CPS makes the CPS unusually polarizable by the SS. For brevity, we only discuss the PBRC and RC calculations here, but we note that the PBRCD and RCD calculations are similar.

Figure 2 shows that for the PBRC calculation employing the SCT scheme, the energy in the embedded-QM calculations drops by 0.88 kcal/mol and 0.17 kcal/mol in the second and the third iterations, respectively. The convergence thresholds (maximum change <0.005 e and root-mean-square change <0.002 e for the charges on the SS atoms in the boundary region) in our tests are modest, because tighter thresholds do not lead to systematically higher accuracy in the QM/MM calculations. The convergence thresholds we used in this study should be adequate for most QM/MM applications where only the energy is important (for example, Monte Carlo calculations¹⁹²), but tighter thresholds may be needed for molecular dynamics calculations requiring gradients.

Figures 3 and 4 illustrate the rapid convergence of the atomic charges for the heavy atoms in the CPS and in the SS in the PBRC calculations employing the SCT scheme.

The charge variations after the second iteration are almost negligible (≤ 0.001 e). As expected, the charge variations in the iterative procedure are more prominent for the CPS atoms close to the QM/MM boundary than for the CPS atoms distant to the QM/MM boundary. The charges on C17 and N18 changed negligibly (<0.001 e) during the whole self-consistent procedure due to shielding effects.

V.B. Case Study of the Atomic Charges. In this subsection, we examine the converged atomic charges resulting from the RC and PBRC calculations. Again we use the Ace-His⁺-NMe system as the example. Although we focus on the RC and PBRC schemes, the conclusions are also applicable to the RCD and PBRCD calculations.

Table 1 shows only small differences between the RC and PBRC calculations of the charges on the CPS atoms. Furthermore, the three treatments (SCT, BT, and EEM) yielded quite similar ESP charges on the CPS atoms in the PBRC calculations. For example, the ESP charge on C13 (which is the Q1 atom) is -0.51 e in the RC calculation, and the charge increases in the PBRC calculations to -0.54 e when employing the SCT treatment or the EEM treatment to -0.57 e when employing the BT treatment. These changes are in the range of 0.03–0.06 e. For the CPS atoms that are distant from the QM/MM boundary, the changes in the charges are even smaller. The small differences in the ESP charges on the CPS atoms between the RC and PBRC calculations and between the three different polarization treatments in the PBRC calculations imply that, for this molecule, the polarization on the CPS by the SS is treated reasonably even in the electrostatic-embedding schemes.

Generally speaking, the ESP charges on the PS atoms in the QM/MM computations agree qualitatively with those in

Table 3. QM/MM Optimized Q1–M1 Bond Distances (Å) in Comparison with Full-QM Results for Small Organic Molecules^a

molecule (SS–PS)	QM ^b	initial charge	RC ^b	PBRC			RCD ^b	PBRCD		
				SCT ^c	BT ^d	EEM		SCT ^c	BT ^d	EEM
CH ₃ –CH ₂ OH	1.527	OPLS-AA	1.519	1.519	1.519	1.519	1.514	1.513	1.513	1.514
		ESP	1.523	1.523	1.523	1.523	1.522	1.521	1.521	1.521
CH ₃ –CH ₂ SH	1.539	OPLS-AA	1.519	1.519	1.519	1.519	1.514	1.514	1.514	1.514
		ESP	1.523	1.523	1.523	1.523	1.521	1.521	1.521	1.521
CH ₃ –CH ₂ NH ₃ ⁺	1.528	OPLS-AA	1.517	1.517	1.517	1.517	1.513	1.513	1.513	1.513
		ESP	1.520	1.520	1.520	1.520	1.519	1.519	1.518	1.519
CH ₃ –CH ₂ COOH	1.533	OPLS-AA	1.521	1.521	1.521	1.521	1.516	1.516	1.516	1.516
		ESP	1.524	1.524	1.524	1.524	1.523	1.523	1.523	1.523
CF ₃ –CH ₂ OH	1.498	OPLS-AA	1.537	1.537	n/a	n/a	1.562	1.562	n/a	n/a
		ESP	1.537	1.537	n/a	n/a	1.558	1.557	n/a	n/a
CH ₂ OH–CH ₂ OH	1.521	OPLS-AA	1.523	1.526	1.524	1.527	1.527	1.529	1.527	1.531
		ESP	1.526	1.527	1.526	1.529	1.531	1.533	1.531	1.534
CH ₂ OH–CH ₂ SH	1.529	OPLS-AA	1.525	1.526	1.525	1.528	1.528	1.530	1.528	1.531
		ESP	1.527	1.528	1.527	1.529	1.532	1.533	1.531	1.534
CH ₃ –CH ₂ O [–]	1.594	OPLS-AA	1.562	1.561	1.561	1.561	1.548	1.548	1.547	1.548
		ESP	1.571	1.571	1.570	1.571	1.567	1.566	1.566	1.567
CH ₃ –CH ₂ S [–]	1.550	OPLS-AA	1.525	1.524	1.524	1.525	1.517	1.516	1.516	1.517
		ESP	1.531	1.530	1.530	1.530	1.528	1.528	1.527	1.528
CH ₃ –CH ₂ NH ₂	1.543	OPLS-AA	1.526	1.526	1.526	1.526	1.519	1.519	1.519	1.519
		ESP	1.530	1.530	1.530	1.530	1.528	1.528	1.528	1.528
CH ₃ –CH ₂ COO [–]	1.533	OPLS-AA	1.527	1.527	1.527	1.527	1.521	1.521	1.521	1.521
		ESP	1.531	1.531	1.531	1.531	1.529	1.529	1.529	1.529
CF ₃ –CH ₂ O [–]	1.521	OPLS-AA	1.617	1.616	n/a	n/a	1.677	1.676	n/a	n/a
		ESP	1.613	1.613	n/a	n/a	1.661	1.659	n/a	n/a
CH ₂ OH–CH ₂ O [–]	1.561	OPLS-AA	1.580	1.587	1.585	1.587	1.591	1.600	1.598	1.599
		ESP	1.587	1.594	1.592	1.593	1.605	1.614	1.613	1.612
CH ₂ OH–CH ₂ S [–]	1.525	OPLS-AA	1.533	1.535	1.533	1.537	1.539	1.541	1.539	1.543
		ESP	1.537	1.538	1.536	1.540	1.546	1.548	1.547	1.550
MUE ^e		OPLS-AA	0.014/0.021	0.015/0.022	0.014	0.015	0.020/0.033	0.021/0.034	0.021	0.021
		ESP	0.012/0.019	0.012/0.020	0.012	0.013	0.016/0.028 ^e	0.017/0.029	0.017	0.017
MSE ^f		OPLS-AA	–0.009/0.002	–0.008/0.003	–0.009	–0.007	–0.11/0.006	–0.010/0.007	–0.011	–0.010
		ESP	–0.004/0.006	–0.004/0.006	–0.004	–0.003	–0.003/0.012	–0.002/0.013	–0.002	–0.001

^a The QM level is HF/MIDI!, and the MM force field is OPLS-AA. The iterative procedure for polarization was initiated by using the OPLS-AA or ESP charges for the embedded-QM calculations. The mean unsigned error (MUE) and mean signed error (MSE) were averaged over the molecules for each QM/MM treatment using the full-QM calculations as standard reference values. ^b Reference 107. ^c QEq model with SCT of Rappé and Goddard. ^d QEq model of Bakowies and Thiel. ^e Mean unsigned error excluding/including CF₃–CH₂OH. ^f Mean signed error excluding/including CF₃–CH₂OH.

Table 4. Proton Affinities (kcal/mol) for Capped Amino Acids^a

molecule	QM	RC	PBRC			PBRCD ^b		PBRCD			PBRCD ^b
			SCT ^c	BT ^d	EEM	SCT ^c	RCD	SCT ^c	BT ^d	EEM	SCT ^c
Ace-Lys-NMe	236.7	234.6	235.7	235.7	235.2	240.3	233.7	234.6	234.4	234.3	238.8
Ace-His ^δ -NMe	251.9	247.3	254.6	242.2	254.5	271.8	246.1	253.2	244.0	252.9	270.5
Ace-His ^ε -NMe	254.7	245.6	251.4	250.5	250.9	269.1	244.3	249.9	248.4	249.8	267.8
Ace-Tyr-NMe	366.8	368.4	363.0	368.3	368.6	348.2	367.2	361.7	366.4	367.6	348.4
Ace-Glu-NMe	358.3	358.0	356.4	357.5	361.2	358.0	356.2	354.4	354.6	359.5	355.3
MUE ^e		3.5	2.5	3.4	2.5	11.4	4.3	3.4	4.1	2.1	11.0
MSE ^f		–2.9	–1.5	–2.8	0.4	3.8	–4.2	–2.9	–4.1	–0.9	2.5

^a The side chain is the PS, and the backbone is the SS (see also Figure 1). The QM level is set to HF/MIDI!, and the MM force field is OPLS-AA. The iterative procedure for polarization was initiated by using the OPLS-AA charges for the embedded-QM calculations. The mean unsigned error (MUE) and the mean signed error (MSE) were averaged over the molecules for each QM/MM treatment using the full-QM calculations as standard reference values. ^b This model allows all SS atoms to change charges. ^c QEq model with SCT of Rappé and Goddard. ^d QEq model of Bakowies and Thiel. ^e Mean unsigned error. ^f Mean signed error.

the full-QM calculations. Bigger discrepancies are seen for the PS atoms close to the QM/MM boundary than for the PS atoms distant from the boundary. But the QM/MM and full-QM calculations yield very different electronic structures for the PS atoms that are close to the QM/MM boundary.

Turning to the SS atoms, we found that in the PBRC calculations the M2 and M3 charges depend strongly on the method of polarization treatment as well as on the parameters used. The BT treatment trends to yield larger charges than the SCT and EEM do. The SCT and EEM schemes gave

Table 5. QM/MM Optimized Q1–M1 Bond Distances (Å) in Comparison with Full-QM Results for Amino Acids^a

molecule	QM	RC	PBRC			RCD	PBRCD		
			SCT ^b	BT ^c	EEM		SCT ^b	BT ^c	EEM
XH or XH ⁺									
Ace-Lys-NMe	1.533	1.542	1.541	1.539	1.540	1.544	1.543	1.541	1.541
Ace-His-NMe	1.558	1.550	1.548	1.546	1.548	1.552	1.550	1.548	1.549
Ace-Tyr-NMe	1.561	1.546	1.547	1.543	1.545	1.549	1.549	1.546	1.548
Ace-Glu-NMe	1.551	1.541	1.540	1.538	1.539	1.543	1.543	1.540	1.541
X ⁻ or X									
Ace-Lys-NMe	1.531	1.543	1.543	1.541	1.542	1.546	1.545	1.544	1.544
Ace-His ^δ -NMe	1.537	1.546	1.545	1.553	1.543	1.549	1.548	1.553	1.543
Ace-His ^ε -NMe	1.559	1.551	1.551	1.549	1.550	1.554	1.554	1.552	1.552
Ace-Tyr-NMe	1.569	1.555	1.556	1.553	1.554	1.560	1.561	1.558	1.558
Ace-Glu-NMe	1.550	1.548	1.549	1.546	1.547	1.551	1.553	1.551	1.550
MUE ^d		0.010	0.009	0.012	0.010	0.009	0.009	0.010	0.009
MSE ^e		−0.003	−0.003	−0.005	−0.005	−0.001	−0.003	−0.002	−0.003

^a The side chain is the PS, and the backbone is the SS (see also Figure 1). The QM level is HF/MIDI!, and the MM force field is OPLS-AA. The iterative procedure for polarization was initiated by using the OPLS-AA charges for the embedded-QM calculations. If not otherwise indicated, only the M2 and M3 atoms in the SS were allowed to change charges. The mean unsigned error (MUE) and the mean signed error (MSE) were averaged over the molecules for each QM/MM treatment using the full-QM calculations as standard reference values. ^b QEq model with SCT of Rappé and Goddard. ^c QEq model of Bakowies and Thiel. ^d Mean unsigned error. ^e Mean signed error.

Table 6. Proton Affinities (kcal/mol) for Amino Acids at the Full-QM Optimized Geometries^a

molecule	QM	RC	PBRC			RCD	PBRCD		
			SCT ^b	BT ^c	EEM		SCT ^b	BT ^c	EEM
Ace-Lys-NMe	236.7	234.0	234.9	235.0	234.1	233.1	233.9	233.7	233.2
Ace-His ^δ -NMe	251.9	241.3	247.6	243.1	246.7	240.1	246.2	240.9	245.6
Ace-His ^ε -NMe	254.7	251.2	256.3	253.6	254.4	250.0	254.9	251.7	253.3
Ace-Tyr-NMe	366.8	368.6	364.0	367.8	368.8	367.3	362.7	365.8	367.7
Ace-Glu-NMe	358.3	363.7	362.1	362.6	366.6	362.0	360.1	359.8	364.9
MUE		4.8	2.9	3.4	3.7	4.9	2.9	3.9	3.7
MSE		-1.9	-0.7	-1.3	0.4	-3.2	-2.1	-3.3	-0.7

^a Single-point QM/MM calculations were carried out at the geometries optimized by full QM. The side chain is the PS, and the backbone is the SS (see also Figure 1). The QM level is HF/MIDI!, and the MM force field is OPLS-AA. The iterative procedure for polarization was initiated by using the OPLS-AA charge parameters as partial atomic charges of SS atoms in the embedded-QM calculations. The mean unsigned error (MUE) and the mean signed error (MSE) were averaged over the molecules for each QM/MM treatment using the full-QM calculations as standard reference data. ^b QEq model with SCT of Rappé and Goddard. ^c QEq model of Bakowies and Thiel.

Table 7. Overall Mean Unsigned Errors (kcal/mol) for Organic Molecules and Capped Amino Acids^a

	PBRC					PBRCD			
	RC	SCT	BT	EEM	RCD	SCT	BT	EEM	
HF/MIDI! ^a	4.9	2.9	3.3	3.6	5.4	4.1	4.4	3.8	
B3LYP/6-31+G ^{*a,b}	4.4	2.1	2.9	3.2	4.5	2.9	3.5	3.3	
MP2/6-31+G ^{*a,c}	4.4	2.2	3.0	3.5	4.5	2.7	3.4	3.4	
overall ^d	4.6	2.4	3.1	3.4	4.8	3.2	3.8	3.5	

^a First the results are averaged over the two choices of unpolarized partial atomic SS charges for the six small organic molecules (excluding 1,1,1-trifluoroethanol) and averaged over the five capped amino acids for the two sets of geometries. Then the results for the small organic molecules and the capped amino acids were each weighted 0.5 for a final average, which is given in the table. ^b See Table S9 in the Supporting Information for proton affinities for small organic molecules and Tables S13 and S15 for proton affinities for capped amino acids. ^c See Table S10 in the Supporting Information for proton affinities for small organic molecules and Tables S16 and S17 for proton affinities for capped amino acids. ^d Average over all three QM levels.

quite similar charges. For example, the charge on the N7 atom was predicted to be -0.41e in the SCT treatment and -0.44 e in the EEM treatment but was predicted to be -0.94 e in the BT treatment. The large charge of -0.94 e seems

unrealistic and may result in an overestimation of the electrostatic interaction between the N7 atom and other atoms.

Although the charges on the SS atoms produced in the PBRC calculations by all the three polarization treatments are in qualitative agreement with the full-QM ESP charges, it is difficult to tell which set of QM/MM charges are more realistic just by comparing them with the full-QM charges. As discussed before, the SS charges enter the QM Hamiltonian of the CPS as one-electron operators. Thus the SS charges are parameters of the effective QM Hamiltonian, and they are not strictly comparable with the full-QM ESP charges or the partial charges in the MM force field, although all the QM (ESP), MM, and QM/MM charges describe the interatomic interactions in their own theoretical frameworks. Which set of parameters are the best parameters depends on the problem one is studying and can only be answered after comparing the calculated molecular properties (e.g., energies and geometries) with standard reference data such as reliable experimental results or highly accurate theoretical calculations.

V.C. Energies and Geometries of Small Organic Molecules. For the optimized Q1–M1 bond distances of the

small organic molecules, including protonated and deprotonated forms (see Table 3), the RC and PBRC calculations yielded almost identical results for the first five molecules. For the last two molecules, $\text{CH}_2\text{OH}-\text{CH}_2\text{OH}$ and $\text{CH}_2\text{OH}-\text{CH}_2\text{SH}$, the differences between the RC and PBRC results are slightly larger: up to 0.004 Å for the neutral species and up to 0.007 Å for the charged species. In comparison with their neutral partners, the charged species were affected more, as expected, by the stronger polarization of the SS due to the charged PS. Different polarization treatments (SCT, BT, and EEM) in the PBRC computations showed negligible differences (typically no more than 0.002 Å) between each other for the Q1–M1 distances. The comparisons between the RCD and PBRCD calculations lead to the same conclusions.

Overall, the polarization of the SS due to the CPS does not change the QM/MM optimized Q1–M1 bond distances significantly. Indeed, the MUE and MSE of Q1–M1 bond distances for the RC (or RCD) calculations are almost the same as those for the PBRC (or PBRCD) calculations with differences of only 0.002 Å or less. Again, we found that the polarization procedure initiated with the ESP charges provided better results for the Q1–M1 bond distances than the polarization procedure initiated with the OPLS-AA charges, just as we saw in the proton affinities.

As indicated in Table 2, the PBRC calculations for the small organic molecules yield noticeable overall improvements in the proton affinities, for which the MUEs (and MSEs) are about 25–60% smaller than the MUE (and MSE) yielded by the RC calculations. The performances by the SCT, BT, and EEM schemes are rather similar, with the MUEs (and MSEs) usually agreeing within 1 kcal/mol. The same trend emerges from the comparisons between the PBRCD and RCD calculations.

The first five molecules in the test suite have no M3 atoms in the SS, and thus for those molecules there is not much freedom for charge variation among the atoms during the polarization procedure. The PBRC and RC proton affinities are very similar to each other with differences usually less than 1 kcal/mol, as are the PBRCD and RCD results. For the last two molecules, the presence of both the M2 and M3 atoms in the SS allows more variational freedom during charge equilibration, and one observes more pronounced improvements in the range of 3–9 kcal/mol.

Interestingly, the polarization treatments initiated with the ESP charges produced better results (with MUEs and MSEs typically 2 kcal/mol smaller) than those initiated with the OPLA-AA charges. The use of the ESP charges, which are generally smaller than the OPLS-AA charges, imposes a smaller Q_{tot} in the charge conservation constraint (eq 12) for the boundary group. The observation of better performance by the ESP charges in this study is consistent with our previous conclusion¹⁰⁷ that the OPLS-AA charges or other charges (e.g., CHARMM or AMBER charge parameters) designed for use in condensed-phase simulations are not very suitable for QM/MM calculations of small molecules in the gas phase.

In order to put the results in perspective it is useful to compare the results in Table 2 to those in ref 107, which

considered the same seven proton affinities (including $\text{CF}_3-\text{CH}_2\text{OH}$). Reference 107 contains results for six treatments not included in Table 2, and they yielded MUEs of 7.1, 5.5, 6.2, 27.4, 14.5, and 8.2 kcal/mol for these seven proton affinities, which may be compared to 3.6 kcal/mol for the PBRC-ESP method and 3.8 kcal/mol for the PBRCD-ESP method. This shows that these new methods are relatively successful, considering the difficulty of the tests. The encouraging improvement demonstrated by the PBRC and PBRCD schemes in comparison with the RC and RCD schemes and the other treatments of ref 107 does not mean that one can use the polarized-embedding schemes without care. The polarized-embedding schemes must be used with caution, as there is no guarantee that the PBRC or PBRCD schemes will give results superior to those by the RC and RCD schemes for all systems. The results depend on the adequacy of the electronegativity equalization scheme and its parameters. Thus, it is recommended that users validate the schemes with a particular parameter set on similar small model systems before applying them to the systems of ultimate interest. In section V.D, we will consider such validation for capped amino acids.

V.D. Energies and Geometries of Capped Amino Acids.

First, we note that, as revealed in Table 4, poor results were produced for proton affinities when all SS atoms were put into a polarizable group and were permitted to vary their charges in the self-consistent polarization procedure. Such an arrangement of the SS atoms in the polarization treatment yielded MUEs of 11 kcal/mol (in both the PBRC and PBRCD calculations); such MUEs are about 3 times as large as the MUEs when only the M2 and M3 atoms were put into the polarizable SS group. Therefore, the scheme of modifying the charges of all SS atoms will not be considered further, and our discussion in the rest of this work will concentrate on the PBRC and PBRCD calculations where only the M2 and M3 atoms were allowed to change their charges.

Table 4 shows that the PBRC and PBRCD calculations using the SCT and EEM parametrizations yield MUEs that are 1–2 kcal/mol smaller than for the RC and RCD calculations, but the PBRC and PBRCD calculations employing the BT parametrization offer only a tiny improvement (0.1 kcal/mol) over the RC and RCD method. Among the three polarization options, the EEM option works best with an MUE of only 2.5 kcal/mol and an MSE of 0.4 kcal/mol in the PBRC calculations and an MUE of 2.1 kcal/mol and an MSE of –0.9 kcal/mol in the PBRCD calculations. The less satisfactory performance of the BT scheme as compared to the SCT and EEM schemes is largely due to the big discrepancies for the histidine deprotonation at the delta position. The proton affinities of Ace-His^δ-NMe calculated by the BT treatment are lower than those calculated by the SCT and EEM treatments by ca. 12 kcal/mol in the PBRC calculations and by ca. 9 kcal/mol in the PBRCD calculations. This is quite unusual, as in the other cases, the SCT, BT, and EEM calculations yield rather similar proton affinities (always <6 kcal/mol and mostly <2 kcal/mol). In particular, the BT proton affinities agree with the SCT and EEM results within 2 kcal/mol for the

Ace-His $^{\epsilon}$ -NMe system, i.e., the histidine deprotonation at the epsilon position, a closely related system.

The large discrepancies in the proton affinities at the delta position for histidine between BT and the other two (SCT and EEM) polarization treatments are due to substantial differences in their optimized geometries. We found that upon the deprotonation at the delta position, the imidazole group bends toward the backbone due to the interaction between the negatively charged N15 atom in the imidazole group and the positively charged H11 atom in the backbone. The BT treatment produces much larger charges on these atoms in Ace-His $^{\delta}$ -NMe than the BT and EEM treatment does. For example, in PBRC calculations, BT yields $Q_{H11} = 0.665$ e and $Q_{N15} = -0.776$ e, while SCT gives $Q_{H11} = 0.269$ e and $Q_{N15} = -0.594$ e, and EEM predicts $Q_{H11} = 0.221$ e and $Q_{N15} = -0.583$ e. The charges in the PBRCD calculations are similar to the charges in the PBRC calculations. The larger charges lead to stronger interactions between N15 and H11. Consequently, the imidazole group is more significantly bent toward the backbone in the BT treatment than in the SCT and EEM treatments. In the BT calculations, the distances between the H11 and N15 are about 1.8 Å in the PBRC calculations and 1.7 Å in the PBRCD calculations, respectively. These distances are much shorter than those given by the SCT and EEM treatments, which were 2.5 Å or longer. The significant differences in geometries contribute to the difference in proton affinities.

The story is different for the histidine deprotonation at the epsilon position. The epsilon position is far away from the backbone atoms, and the N18 atom does not interact closely with the backbone atoms. Moreover, the charge on the H21 atom that is bonded to the N15 atom is also positive; the H21 atom is present in the Ace-His $^{\epsilon}$ -NMe and the Ace-His $^{+}$ -NMe systems but absent in the Ace-His $^{\delta}$ -NMe system. The repulsion between H21 and H11 in the Ace-His $^{\epsilon}$ -NMe model did not induce the same geometric changes (the bending of the imidazole group) as one observed in the Ace-His $^{\delta}$ -NMe model. Actually the distance between H11 and H21 barely change upon deprotonation at the epsilon position: they increased from about 3.9–4.0 Å in Ace-His $^{+}$ -NMe to about 4.1–4.2 Å in the Ace-His $^{\epsilon}$ -NMe. As expected, the conformations for all three polarization treatments are very close to each other, and the proton affinities were calculated to be quite similar.

The above explanations are confirmed by the QM/MM//full-QM proton affinities given in Table 6. The use of the same full-QM geometries eliminates the discrepancies due to different geometries, and we indeed found relatively small (<5 kcal/mol) variations between proton affinities calculated by all three treatments. In comparison with the QM/MM proton affinities, the overall variations in the QM/MM//full-QM proton affinities are reduced by about 50%.

For the QM/MM optimized Q1–M1 bond distances, as shown in Table 5, the performances of all three polarization treatments resemble their performance for proton affinities. They all give MUEs of about 0.01 Å and MSEs no larger than 0.005 Å, which are acceptably small for a variety of applications.

V.E. Other QM Methods. Additional calculations using the B3LYP/6-31+G* and MP2/6-31+G* levels of theory are given in the Supporting Information Tables S8–S19.

Comparing the proton affinities for small organic molecules listed in Table 2 (QM = HF/MIDI!), in Table S9 (QM = B3LYP/6-31+G*), and in Table S11 (QM = MP2/6-31+G*), there are no large changes in the accuracy in energy when different QM methods are employed for a given (polarizable) boundary treatment. Generally speaking, B3LYP/6-31+G* produces the best results, and HF/MIDI! shows the largest errors. Inspection of the Q1–M1 bond length in Tables 3, S10, and S12 gives similar conclusions. Turn to the capped amino acids, all three QM levels gave quite comparable results for proton affinities (Tables S13 and S15 for QM = DFT and Tables S16 and S17 for QM = MP2 calculations), and it is hard to tell which is superior to the others. Thus, all these additional calculations support our conclusions: Inclusion of the mutual polarization yields improves the QM/MM proton affinities for all the three QM levels in our test, and the extents of improvement are rather similar for all three levels. Inclusion of the mutual polarization leads to little change in the geometry. Interestingly, the ESP charges seem to always perform better than OPLS-AA charges for small organic compound.

V.F. Overall Assessment and Future Work. Table 7 presents an overall energetic assessment of the performance of the new polarized-boundary methods and the unpolarized boundaries from which they were evolved. This table is based on the proton affinities for the 11 cases (six organic molecules and five capped amino acids) where parameters are available for all methods examined. In general, in the ultimate applications, if some atoms close to the QM/MM boundary are found to undergo significant polarization effects, they should, if possible, be included into the QM subsystems; however, for testing a method to see if it is robust, it is instructive to push the envelope. That is why we included a few difficult cases in our test suite; for example, in CF₃–CH₂OH the bond breaking is occurring at a place very close to the QM/MM boundary, and MM atoms carrying large partial charges are located near the boundary. This particular molecule is included in Tables 2 and 3 but not in Table 7. Nevertheless, we see that the mean unsigned error of the most successful method without boundary polarization is ca. 5 kcal/mol, but that this is reduced to ca. 3 kcal/mol by four of the six methods with boundary polarization. On one hand, this shows the importance of boundary polarization, and the reduction of the error by 40% is encouraging. On the other hand, even though these are very challenging tests (adding a whole charge very close to the boundary), one might have hoped that the mean unsigned error would be reduced even further. One remaining source of error is that the present treatment assumes no charge transfer between the PS and the SS, even though the PS and SS are covalently bonded.

In principle, the interactions between the PS and SS can be modeled more realistically if one allows fractional (or whole) charges to be transferred between the PS and SS. Such a treatment could be called flexible-boundary QM/MM (FB-QM/MM, FBRC, or FBRCD). For FB-QM/MM calcu-

lations one needs an algorithm that describes the electronic structure of a system with fractional electrons and provides a prescription for how much charge should be transferred. Gogonea and Merz^{193,194} have proposed a combined quantum mechanical-Poisson-Boltzmann equation approach to study the charge transfer between ions and a solvent medium treated as a dielectric continuum. In their treatment, the charge being transferred is represented by a surface charge density at the dielectric interface, which modifies the boundary condition for which the Poisson-Boltzmann equation is solved. The ions are described by an effective QM Hamiltonian that resembles Dewar's half-electron method^{195,196} but with subtle differences in handling the electron-electron repulsion term. The self-consistent QM calculations are carried out in terms of the density matrix by adding electron density to the LUMO (in the case of charge transferred to ions) or by subtracting electron density from the HOMO (in the case of charge transferred to solvent). The amount of charge being transferred is determined variationally subject to the criterion of the free energy including the environment. Sprik and co-workers¹⁹⁷ proposed another scheme that can potentially be used to handle fractional charge transfer between the PS and SS in the QM/MM calculations. They model the exchange of electrons between molecule and a reservoir of fixed chemical potential by a modification of the Car-Parrinello¹⁹⁸ method allowing for fluctuating numbers of electrons under constraints of fixed electronic chemical potential. They adopted an approach involving multiple diabatic potentials energy surfaces where each surface corresponds to a system with a strictly integer number of electrons, e.g., a surface for the reduced state whose charge is 0 and a surface for the oxidized state whose charge is +1 e. Thermochemical properties in a molecular dynamics run were computed by a weighted average of the partition functions for the two oxidation states; in other words, one avoids treating a fractional number of electrons by moving the system on an effective (adiabatic) potential that is a weighted average of diabatic potential surfaces corresponding to integer numbers of electrons. The weights are determined by the chemical potential and the mole fraction of the cations. This provides a more justifiable treatment of electron exchange, but it has been criticized because of the need for a uniform background charge.¹⁹⁹ Further research on FB-QM/MM would be valuable.

VI. Summary and Conclusions

In this work, we developed two polarized boundary embedding schemes, the PBRC and PBRCD schemes, to allow a more accurate treatment of QM/MM boundaries. The newly developed schemes combine the electrostatic-embedding RC and RCD schemes,¹⁰⁷ where the CPS is polarized by the SS, with an electronegativity-equalization or charge-equilibration scheme to describe the polarization of the boundary region of the SS by the CPS. More specifically, in the PBRC and PBRCD schemes, the polarization of the SS by the CPS is realized by adjusting the point charges at the SS atomic sites in the embedded-QM calculations. The calculations were carried out with a new version of the QMMM computer program¹⁸⁰ that is general enough to handle cases where the

QM-MM boundary passes between molecules (as in the earlier work of Field²⁷) or when it passes through a covalent bond. For either type of boundary, the QMMM computer program is also general enough to polarize only one group of the SS, to polarize two or more defined groups, or to polarize the whole SS as a single group. We focus in this paper though on the PBRC and PBRCD schemes where the boundary passes through a covalent bond and only one group, in particular the boundary group, of the SS is polarized.

In this work, the implementation polarization of the SS by the CPS is based on the principle of electronegativity equalization or charge equilibration. The advantage of this scheme is that it is simple and easy to implement. Moreover, the polarization effects expressed in the charge redistribution are easy to interpret. Although variation of atomic charges does not account for all polarization effects,¹⁴⁰ in most applications, the variation of charges based on electronegativity equalization is probably adequate to account for the dominant polarization effect on the boundary region of the SS.

For the determination of the charges on the SS atoms, we implemented both the QEq¹⁵³ and EEM¹⁵¹ methods with modifications to take into account the external electric field generated by the CPS and by the unpolarized part of the SS. In the QEq calculations we employed the empirical functions and parameter sets of both Rappé and Goddard¹⁵³ and Bakowies and Thiel¹⁷ to compute interatomic electrostatic interactions. Self-consistency in the mutual polarization of the CPS and the SS is accomplished by an iterative procedure; usually convergence is achieved within three sets of iterations.

If there is no significant charge transfer involved, due to the cancellation of errors in the reactant state and the errors in the product state, good energetics might be obtained by using the electrostatic-embedding schemes where only the CPS is polarized by the SS or even by using the mechanical-embedding scheme where the electrostatic interactions between the CPS and the SS are handled at the MM level. The electronic structures of the CPS will be different in the polarized-embedding schemes, in the electrostatic-embedding schemes, and in the mechanical-embedding schemes. However, as indicated by the ESP charges for the CPS in section V.B., the difference in the electronic structures of the CPS is often small between the polarized-embedding calculations and the electrostatic-embedding calculations. Therefore, in many applications, it is probably sufficient to use the electrostatic-embedding methods. However, the mutual polarization of the CPS and SS is expected to be important in situations where significant charge-transfer takes place in the CPS during a reaction, e.g., the protonation reactions we investigated in the present study. Therefore the PBRC and PBRCD schemes were tested by calculating proton affinities for small organic molecules and capped amino acids. The proton affinity is a critical test for QM/MM methods because of the significant changes in the charges of the CPS upon protonation; thus proton affinities are very sensitive to the treatment of electrostatic interactions between the CPS and SS and are likely to show prominent polarization effects in the SS. We found that there is no significant difference in

the Q1–M1 bond distances between the calculations with and without polarization of the boundary region of the SS, but encouraging improvement in the computed proton affinities was obtained by the new methods in comparison with the errors of RC and RCD calculations that did not consider the polarization of the SS by the CPS (and also in comparison with even larger errors obtained in other treatments considered in a previous paper). These findings suggest the importance of the mutual polarization of the CPS and SS in QM/MM calculations where charge transfers occur in the CPS, and the success of the new polarization treatment implemented here in handling the polarization of the SS is gratifying.

Acknowledgment. This work is supported by the Research Corporation through the award no. CC6725 to H. Lin and by the Office of Naval Research under award no. N00014-05-1-0538 to D. G. Truhlar. We thank the Advanced Biomedical Computing Center and the Minnesota Supercomputing Institute for providing CPU time and access to the *Gaussian03* program.

Supporting Information Available: QEq and EEM parameters in the present study taken from the literature (Table S1), nonstandard MM parameters in this work in the TINKER parameter file format (Table S2), atom types, full-QM optimized coordinates, and connectivities of the capped amino acids in the test suite (in the *tinker.xyz* file format) (Table S3), atomic charges derived from the full-QM and selected QM/MM calculations for the capped amino acids (Table S4), convergence of the atomic charges of the heavy atoms in the PS and SS and of embedded-QM energies for the CPS in the PBRC calculations employing the SCT parameters for the Ace-His⁺-NMe system and its deprotonated forms (Table S5), comparison of the charges on H11, H21, and N15 and distances between H11 and H21 and between H11 and N15 for the Ace-His⁺-NMe system and its deprotonated forms (Table S6), atomic charges derived from the full-QM and selected QM/MM calculations for the capped amino acids at the full-QM optimized geometries (Table S7), and effect of changing the quantum mechanical level, as discussed in section V.E (Tables S8–S19). This material is available free of charge via the Internet at <http://pubs.acs.org>.

References

- (1) Warshel, A.; Levitt, M. *J. Mol. Biol.* **1976**, *103*, 227.
- (2) Bacalis, N. C.; Kunz, A. B. *Phys. Rev. B: Condens. Matter* **1985**, *32*, 4857.
- (3) Singh, U. C.; Kollmann, P. A. *J. Comput. Chem.* **1986**, *7*, 718.
- (4) Barandiaran, Z.; Seijo, L. *J. Chem. Phys.* **1988**, *89*, 5739.
- (5) Field, M. J.; Bash, P. A.; Karplus, M. *J. Comput. Chem.* **1990**, *11*, 700.
- (6) Ferenczy, G. G.; Rivail, J.-L.; Surjan, P. R.; Naray-Szabo, G. *J. Comput. Chem.* **1992**, *13*, 830.
- (7) Gao, J.; Xia, X. *Science* **1992**, *258*, 631.
- (8) Åqvist, J.; Warshel, A. *Chem. Rev.* **1993**, *93*, 2523.
- (9) Thery, V.; Rinaldi, D.; Rivail, J.-L.; Maigret, B.; Ferenczy, G. G. *J. Comput. Chem.* **1994**, *15*, 269.
- (10) Thompson, M. A.; Glendenning, E. D.; Feller, D. *J. Phys. Chem.* **1994**, *98*, 10465.
- (11) Maseras, F.; Morokuma, K. *J. Comput. Chem.* **1995**, *16*, 1170.
- (12) Stanton, R. V.; Hartsough, D. S.; Merz, K. M., Jr. *J. Comput. Chem.* **1995**, *16*, 113.
- (13) Thompson, M. A. *J. Phys. Chem.* **1995**, *99*, 4794.
- (14) Thompson, M. A.; Schenter, G. K. *J. Phys. Chem.* **1995**, *99*, 6374.
- (15) Assfeld, X.; Rivail, J.-L. *Chem. Phys. Lett.* **1996**, *263*, 100.
- (16) Bakowies, D.; Thiel, W. *J. Phys. Chem.* **1996**, *100*, 10580.
- (17) Bakowies, D.; Thiel, W. *J. Comput. Chem.* **1996**, *17*, 87.
- (18) Barnes, J. A.; Williams, I. H. *Biochem. Soc. Trans.* **1996**, *24*, 263.
- (19) Day, P. N.; Jensen, J. H.; Gordon, M. S.; Webb, S. P.; Stevens, W. J.; Krauss, M.; Garmer, D.; Basch, H.; Cohen, D. *J. Chem. Phys.* **1996**, *105*, 1968.
- (20) Eichler, U.; Kölmel, C. M.; Sauer, J. *J. Comput. Chem.* **1996**, *18*, 463.
- (21) Eurenus, K. P.; Chatfield, D. C.; Brooks, B. R.; Hodoscek, M. *Int. J. Quantum Chem.* **1996**, *60*, 1189.
- (22) Gao, J. *Rev. Comput. Chem.* **1996**, *7*, 119.
- (23) Kerdcharoen, T.; Liedl, K. R.; Rode, B. M. *Chem. Phys.* **1996**, *211*, 313.
- (24) Svensson, M.; Humbel, S.; Froese, R. D. J.; Matsubara, T.; Sieber, S.; Morokuma, K. *J. Phys. Chem.* **1996**, *100*, 19357.
- (25) Bersuker, I. B.; Leong, M. K.; Boggs, J. E.; Pearlman, R. S. *Int. J. Quantum Chem.* **1997**, *63*, 1051.
- (26) Cummins, P. L.; Gready, J. E. *J. Comput. Chem.* **1997**, *18*, 1496.
- (27) Field, M. J. *Mol. Phys.* **1997**, *91*, 835.
- (28) Gao, J. *J. Comput. Chem.* **1997**, *18*, 1061.
- (29) Gao, J.; Alhambra, C. *J. Chem. Phys.* **1997**, *107*, 1212.
- (30) Pascual, J.; Pettersson, L. G. M. *Chem. Phys. Lett.* **1997**, *270*, 351.
- (31) Sherwood, P.; De Vries, A. H.; Collins, S. J.; Greatbanks, S. P.; Burton, N. A.; Vincent, M. A.; Hillier, I. H. *Faraday Discuss.* **1997**, *106*, 79.
- (32) Bryce, R. A.; Vincent, M. A.; Malcolm, N. O. J.; Hillier, I. H.; Burton, N. A. *J. Chem. Phys.* **1998**, *109*, 3077.
- (33) Gao, J.; Amara, P.; Alhambra, C.; Field, M. J. *J. Phys. Chem. A* **1998**, *102*, 4714.
- (34) Kaminski, G. A.; Jorgensen, W. L. *J. Phys. Chem. B* **1998**, *102*, 1787.
- (35) Mordasini, T.; Thiel, W. *Chimia* **1998**, *52*, 288.
- (36) Sinclair, P. E.; de Vries, A.; Sherwood, P.; Catlow, C. R. A.; van Santen, R. A. *J. Chem. Soc., Faraday Trans.* **1998**, *94*, 3401.
- (37) Stefanovich, E. V.; Truong, T. N. *J. Phys. Chem. B* **1998**, *102*, 3018.
- (38) Tongraar, A.; Liedl, K. R.; Rode, B. M. *J. Phys. Chem. A* **1998**, *102*, 10340.

- (39) Woo, T. K.; Cavallo, L.; Ziegler, T. *Theor. Chem. Acc.* **1998**, *100*, 307.
- (40) Antes, I.; Thiel, W. *J. Phys. Chem. A* **1999**, *103*, 9290.
- (41) Dapprich, S.; Komáromi, I.; Byun, K. S.; Morokuma, K.; Frisch, M. J. *THEOCHEM* **1999**, 461–462, 1.
- (42) Eichinger, M.; Tavan, P.; Hutter, J.; Parrinello, M. *J. Chem. Phys.* **1999**, *110*, 10452.
- (43) Hillier, I. H. *THEOCHEM* **1999**, 463, 45.
- (44) Lyne, P. D.; Hodoscek, M.; Karplus, M. *J. Phys. Chem. A* **1999**, *103*, 3462.
- (45) Monard, G.; Merz, K. M., Jr. *Acc. Chem. Res.* **1999**, *32*, 904.
- (46) Philipp, D. M.; Friesner, R. A. *J. Comput. Chem.* **1999**, *20*, 1468.
- (47) Pitarch, J.; Pascual-Ahuir, J. L.; Silla, E.; Tunon, I.; Ruiz-Lopez, M. F. *J. Comput. Chem.* **1999**, *20*, 1401.
- (48) Shoemaker, J. R.; Burggraf, L. W.; Gordon, M. S. *J. Phys. Chem. A* **1999**, *103*, 3245.
- (49) Turner, A. J.; Moliner, V.; Williams, I. H. *Phys. Chem. Chem. Phys.* **1999**, *1*, 1323.
- (50) Zhang, Y.; Lee, T.-S.; Yang, W. *J. Chem. Phys.* **1999**, *110*, 46.
- (51) Amara, P.; Field, M. J.; Alhambra, C.; Gao, J. *Theor. Chem. Acc.* **2000**, *104*, 336.
- (52) Cui, Q.; Karplus, M. *J. Chem. Phys.* **2000**, *112*, 1133.
- (53) Cui, Q.; Karplus, M. *J. Phys. Chem. B* **2000**, *104*, 3721.
- (54) Derenzo, S. E.; Klintenberg, M. K.; Weber, M. J. *J. Chem. Phys.* **2000**, *112*, 2074.
- (55) Gogonea, V.; Westerhoff, L. M.; Merz, K. M., Jr. *J. Chem. Phys.* **2000**, *113*, 5604.
- (56) Hall, R. J.; Hindle, S. A.; Burton, N. A.; Hillier, I. H. *J. Comput. Chem.* **2000**, *21*, 1433.
- (57) Hammes-Schiffer, S. *Acc. Chem. Res.* **2000**, *34*, 273.
- (58) Kairys, V.; Jensen, J. H. *J. Phys. Chem. A* **2000**, *104*, 6656.
- (59) Luque, F. J.; Reuter, N.; Cartier, A.; Ruiz-López, M. F. *J. Phys. Chem. A* **2000**, *104*, 10923.
- (60) Murphy, R. B.; Philipp, D. M.; Friesner, R. A. *J. Comput. Chem.* **2000**, *21*, 1442.
- (61) Murphy, R. B.; Philipp, D. M.; Friesner, R. A. *Chem. Phys. Lett.* **2000**, *321*, 113.
- (62) Reuter, N.; Dejaegere, A.; Maigret, B.; Karplus, M. *J. Phys. Chem. A* **2000**, *104*, 1720.
- (63) Röthlisberger, U.; Carloni, P.; Doclo, K.; Parrinello, M. *J. Bio. Inorg. Chem.* **2000**, *5*, 236.
- (64) Sauer, J.; Sierka, M. *J. Comput. Chem.* **2000**, *21*, 1470.
- (65) Sherwood, P. In *Modern Methods and Algorithms of Quantum Chemistry*; Grotendorst, J., Ed.; NIC-Directors: Princeton, 2000; Vol. 3, pp 285.
- (66) Sierka, M.; Sauer, J. *J. Chem. Phys.* **2000**, *112*, 6983.
- (67) Sushko, P. V.; Shluger, A. L.; Catlow, C. R. A. *Surf. Sci.* **2000**, *450*, 153.
- (68) Cui, Q.; Elstner, M.; Kaxiras, E.; Frauenheim, T.; Karplus, M. *J. Phys. Chem. B* **2001**, *105*, 569.
- (69) Nasluzov, V. A.; Rivanenkov, V. V.; Gordienko, A. B.; Neyman, K. M.; Birkenheuer, U.; Rösch, N. *J. Chem. Phys.* **2001**, *115*, 8157.
- (70) Nicoll, R. M.; Hindle, S. A.; MacKenzie, G.; Hillier, I. H.; Burton, N. A. *Theor. Chem. Acc.* **2001**, *106*, 105.
- (71) Poteau, R.; Ortega, I.; Alary, F.; Solis, A. R.; Barthelat, J. C.; Daudey, J. P. *J. Phys. Chem. A* **2001**, *105*, 198.
- (72) Vreven, T.; Mennucci, B.; da Silva, C. O.; Morokuma, K.; Tomasi, J. *J. Chem. Phys.* **2001**, *115*, 62.
- (73) Batista, E. R.; Friesner, R. A. *J. Phys. Chem. B* **2002**, *106*, 8136.
- (74) Colombo, M. C.; Guidoni, L.; Laio, A.; Magistrato, A.; Maurer, P.; Piana, S.; Rohrig, U.; Spiegel, K.; Sulpizi, M.; VandeVondele, J.; Zumstein, M.; Röthlisberger, U. *Chimia* **2002**, *56*, 13.
- (75) Das, D.; Eurenium, K. P.; Billings, E. M.; Sherwood, P.; Chatfield, D. C.; Hodoscek, M.; Brooks, B. R. *J. Chem. Phys.* **2002**, *117*, 10534.
- (76) DiLabio, G. A.; Hurley, M. M.; Christiansen, P. A. *J. Chem. Phys.* **2002**, *116*, 9578.
- (77) Ferré, N.; Assfeld, X.; Rivail, J.-L. *J. Comput. Chem.* **2002**, *23*, 610.
- (78) Gao, J.; Truhlar, D. G. *Annu. Rev. Phys. Chem.* **2002**, *53*, 467.
- (79) Gogonea, V. *Internet Electron. J. Mol. Des.* **2002**, *1*, 173.
- (80) Kerdcharoen, T.; Morokuma, K. *Chem. Phys. Lett.* **2002**, *355*, 257.
- (81) Laio, A.; VandeVondele, J.; Röthlisberger, U. *J. Chem. Phys.* **2002**, *116*, 6941.
- (82) Morokuma, K. *Philos. Trans. R. Soc. London, Ser. A* **2002**, *360*, 1149.
- (83) Schöneboom, J. C.; Lin, H.; Reuter, N.; Thiel, W.; Cohen, S.; Ogliaro, F.; Shaik, S. *J. Am. Chem. Soc.* **2002**, *124*, 8142.
- (84) Titmuss, S. J.; Cummins, P. L.; Rendell, A. P.; Bliznyuk, A. A.; Gready, J. E. *J. Comput. Chem.* **2002**, *23*, 1314.
- (85) Truhlar, D. G.; Gao, J.; Alhambra, C.; Garcia-Viloca, M.; Corchado, J.; Sanchez, M. L.; Villa, J. *Acc. Chem. Res.* **2002**, *35*, 341.
- (86) Amara, P.; Field, M. J. *Theor. Chem. Acc.* **2003**, *109*, 43.
- (87) Devi-Kesavan, L. S.; Garcia-Viloca, M.; Gao, J. *Theor. Chem. Acc.* **2003**, *109*, 133.
- (88) Dinner, A. R.; Lopez, X.; Karplus, M. *Theor. Chem. Acc.* **2003**, *109*, 118.
- (89) Hu, H.; Elstner, M.; Hermans, J. *Proteins: Struct., Funct., Genet.* **2003**, *50*, 451.
- (90) Kongsted, J.; Osted, A.; Mikkelsen, K. V.; Christiansen, O. *J. Phys. Chem. A* **2003**, *107*, 2578.
- (91) Li, G.; Zhang, X.; Cui, Q. *J. Phys. Chem. B* **2003**, *107*, 8643.
- (92) Lofler, M. J.; Loeffler, H. H.; Liedl, K. R. *J. Comput. Chem.* **2003**, *24*, 1240.
- (93) Molina, P. A.; Sikorski, R. S.; Jensen, J. H. *Theor. Chem. Acc.* **2003**, *109*, 100.
- (94) Mordasini, T.; Curioni, A.; Andreoni, W. *J. Biol. Chem.* **2003**, *278*, 4381.

- (95) Sherwood, P.; de Vries, A. H.; Guest, M. F.; Schreckenbach, G.; Catlow, C. R. A.; French, S. A.; Sokol, A. A.; Bromley, S. T.; Thiel, W.; Turner, A. J.; Billeter, S.; Terstegen, F.; Thiel, S.; Kendrick, J.; Rogers, S. C.; Casci, J.; Watson, M.; King, F.; Karlsen, E.; Sjøvoll, M.; Fahmi, A.; Schafer, A.; Lennartz, C. *THEOCHEM* **2003**, 632, 1.
- (96) Sulpizi, M.; Laio, A.; VandeVondele, J.; Cattaneo, A.; Röthlisberger, U.; Carloni, P. *Proteins: Struct., Funct., Genet.* **2003**, 52, 212.
- (97) Swart, M. *Int. J. Quantum Chem.* **2003**, 91, 177.
- (98) Tresadern, G.; Faulder, P. F.; Gleeson, M. P.; Tai, Z.; MacKenzie, G.; Burton, N. A.; Hillier, I. H. *Theor. Chem. Acc.* **2003**, 109, 108.
- (99) Vreven, T.; Morokuma, K.; Farkas, O.; Schlegel, H. B.; Frisch, M. J. *J. Comput. Chem.* **2003**, 24, 760.
- (100) Yang, W.; Drueckhammer, D. G. *J. Phys. Chem. B* **2003**, 107, 5986.
- (101) Laio, A.; Gervasio, F. L.; VandeVondele, J.; Sulpizi, M.; Röthlisberger, U. *J. Phys. Chem. B* **2004**, 108, 7963.
- (102) Pu, J.; Gao, J.; Truhlar, D. G. *J. Phys. Chem. A* **2004**, 108, 632.
- (103) Pu, J.; Gao, J.; Truhlar, D. G. *J. Phys. Chem. A* **2004**, 108, 5454.
- (104) Riccardi, D.; Li, G. H.; Cui, Q. *J. Phys. Chem. B* **2004**, 108, 6467.
- (105) Gregersen, B. A.; York, D. M. *J. Phys. Chem. B* **2005**, 109, 536.
- (106) König, P. H.; Hoffmann, M.; Frauenheim, T.; Cui, Q. *J. Phys. Chem. B* **2005**, 109, 9082.
- (107) Lin, H.; Truhlar, D. G. *J. Phys. Chem. A* **2005**, 109, 3991.
- (108) Nam, K.; Gao, J.; York, D. M. *J. Chem. Theory Comput.* **2005**, 1, 2.
- (109) Pu, J.; Gao, J.; Truhlar, D. G. *ChemPhysChem* **2005**, 6, 1853.
- (110) Wanko, M.; Hoffmann, M.; Strodel, P.; Koslowski, A.; Thiel, W.; Neese, F.; Frauenheim, T.; Elstner, M. *J. Phys. Chem. B* **2005**, 109, 3606.
- (111) Zhang, Y. *J. Chem. Phys.* **2005**, 122, 024114.
- (112) Cisneros, G. A.; Piquemal, J.-P.; Darden, T. A. *J. Phys. Chem. B* **2006**, 110, 13682.
- (113) Fornili, A.; Loos, P.-F.; Sironi, M.; Assfeld, X. *Chem. Phys. Lett.* **2006**, 427, 236.
- (114) Illingworth, C. J. R.; Gooding, S. R.; Winn, P. J.; Jones, G. A.; Ferenczy, G. G.; Reynolds, C. A. *J. Phys. Chem. A* **2006**, 110, 6487.
- (115) Mallik, A.; Taylor, D. E.; Runge, K.; Dufty, J. W.; Cheng, H.-P. *J. Comput.-Aided Mater. Des.* **2006**, 13, 45.
- (116) Riccardi, D.; Schaefer, P.; Yang, Y.; Yu, H.; Ghosh, N.; Prat-Resina, X.; König, P.; Li, G.; Xu, D.; Guo, H.; Elstner, M.; Cui, Q. *J. Phys. Chem. B* **2006**, 110, 6458.
- (117) (a) Vreven, T.; Frisch, M. J.; Kudin, K. N.; Schlegel, H. B.; Morokuma, K. *Mol. Phys.* **2006**, 104, 701. (b) Vreven, T.; Byun, K. S.; Komromi, I.; Dapprich, S.; Montgomery, J. A., Jr.; Morokuma, K.; Frisch, M. J. *J. Chem. Theory Comput.* **2006**, 2, 815.
- (118) (a) Raff, L. M. *J. Chem. Phys.* **1974**, 60, 2220. (b) Joseph, T.; Steckler, R.; Truhlar, D. G. *J. Chem. Phys.* **1987**, 87, 7036. (c) Chakraborty, A.; Zhao, Y.; Lin, H.; Truhlar, D. G. *J. Chem. Phys.* **2006**, 124, 44315.
- (119) Lin, H.; Truhlar, D. G. *Theor. Chem. Acc.* **2007**, 117, 185.
- (120) Heyden, A.; Lin, H.; Truhlar, D. G. *J. Phys. Chem. B* **2007**, 111, 2231.
- (121) Cornell, W. D.; Cieplak, P.; Bayly, C. I.; Gould, I. R.; Merz, K. M., Jr.; Ferguson, D. M.; Spellmeyer, D. C.; Fox, T.; Caldwell, J. W.; Kollman, P. A. *J. Am. Chem. Soc.* **1995**, 117, 5179.
- (122) MacKerell, A. D., Jr.; Bashford, D.; Bellott, M.; Dunbrack, R. L.; Evanseck, J. D.; Field, M. J.; Fischer, S.; Gao, J.; Guo, H.; Ha, S.; Joseph-McCarthy, D.; Kuchnir, L.; Kuczera, K.; Lau, F. T. K.; Mattos, C.; Michnick, S.; Ngo, T.; Nguyen, D. T.; Prodhom, B.; Reiher, W. E., III; Roux, B.; Schlenkrich, M.; Smith, J. C.; Stote, R.; Straub, J.; Watanabe, M.; Wiorkiewicz-Kuczera, J.; Yin, D.; Karplus, M. *J. Phys. Chem. B* **1998**, 102, 3586.
- (123) Jorgensen, W. L.; Maxwell, D. S.; Tirado-Rives, J. *J. Am. Chem. Soc.* **1996**, 118, 11225.
- (124) Jorgensen, W. L.; McDonald, N. A. *THEOCHEM* **1998**, 424, 145.
- (125) McDonald, N. A.; Jorgensen, W. L. *J. Phys. Chem. B* **1998**, 102, 8049.
- (126) Rizzo, R. C.; Jorgensen, W. L. *J. Am. Chem. Soc.* **1999**, 121, 4827.
- (127) Kaminski, G. A.; Friesner, R. A.; Tirado-Rives, J.; Jorgensen, W. L. *J. Phys. Chem. B* **2001**, 105, 6474.
- (128) Kahn, K.; Bruice, T. C. *J. Comput. Chem.* **2002**, 23, 977.
- (129) Frisch, M. J.; Trucks, G. W.; Schlegel, H. B.; Scuseria, G. E.; Robb, M. A.; Cheeseman, J. R.; Montgomery, J. A., Jr.; Vreven, T.; Kudin, K. N.; Burant, J. C.; Millam, J. M.; Iyengar, S. S.; Tomasi, J.; Barone, V.; Mennucci, B.; Cossi, M.; Scalmani, G.; Rega, N.; Petersson, G. A.; Nakatsuji, H.; Hada, M.; Ehara, M.; Toyota, K.; Fukuda, R.; Hasegawa, J.; Ishida, M.; Nakajima, T.; Honda, Y.; Kitao, O.; Nakai, H.; Klene, M.; Li, X.; Knox, J. E.; Hratchian, H. P.; Cross, J. B.; Adamo, C.; Jaramillo, J.; Gomperts, R.; Stratmann, R. E.; Yazyev, O.; Austin, A. J.; Cammi, R.; Pomelli, C.; Ochterski, J. W.; Ayala, P. Y.; Morokuma, K.; Voth, G. A.; Salvador, P.; Dannenberg, J. J.; Zakrzewski, V. G.; Dapprich, S.; Daniels, A. D.; Strain, M. C.; Farkas, O.; Malick, D. K.; Rabuck, A. D.; Raghavachari, K.; Foresman, J. B.; Ortiz, J. V.; Cui, Q.; Baboul, A. G.; Clifford, S.; Cioslowski, J.; Stefanov, B. B.; Liu, G.; Liashenko, A.; Piskorz, P.; Komaromi, I.; Martin, R. L.; Fox, D. J.; Keith, T.; Al-Laham, M. A.; Peng, C. Y.; Nanayakkara, A.; Challacombe, M.; Gill, P. M. W.; Johnson, B.; Chen, W.; Wong, M. W.; Gonzalez, C.; Pople, J. A. *Gaussian03*; Gaussian, Inc.: Pittsburgh, PA, 2003.
- (130) Neese, F. *ORCA, Version 2.4 ed.*; Max Planck Institute for Bioinorganic Chemistry: Muelheim/Ruhr, 2006.
- (131) Price, S. L.; Stone, A. J. *J. Chem. Soc., Faraday Trans.* **1992**, 88, 1755.
- (132) Koch, U.; Popelier, P. L. A.; Stone, A. J. *Chem. Phys. Lett.* **1995**, 238, 253.
- (133) Matta, C. F.; Bader, R. F. W. *Proteins: Struct., Funct., Genet.* **2000**, 40, 310.
- (134) Minikis, R. M.; Kairys, V.; Jensen, J. H. *J. Phys. Chem. A* **2001**, 105, 3829.
- (135) Dick, B. G., Jr.; Overhauser, A. W. *Phys. Rev.* **1958**, 112, 90.
- (136) Stillinger, F. H.; David, C. W. *J. Chem. Phys.* **1978**, 69, 1473.

- (137) Sprik, M.; Klein, M. L. *J. Chem. Phys.* **1988**, *89*, 7556.
- (138) Dang, L. X.; Rice, J. E.; Caldwell, J.; Kollman, P. A. *J. Am. Chem. Soc.* **1991**, *113*, 2481.
- (139) Dang, L. X. *J. Chem. Phys.* **1992**, *97*, 2659.
- (140) Rick, S. W.; Stuart, S. J.; Berne, B. J. *J. Chem. Phys.* **1994**, *101*, 6141.
- (141) Kowall, T.; Foglia, F.; Helm, L.; Merbach, A. E. *J. Am. Chem. Soc.* **1995**, *117*, 3790.
- (142) Banks, J. L.; Kaminski, G. A.; Zhou, R.; Mainz, D. T.; Berne, B. J.; Friesner, R. A. *J. Chem. Phys.* **1999**, *110*, 741.
- (143) Stern, H. A.; Kaminski, G. A.; Banks, J. L.; Zhou, R.; Berne, B. J.; Friesner, R. A. *J. Phys. Chem. B* **1999**, *103*, 4730.
- (144) Martinez, J. M.; Hernandez-Cobos, J.; Saint-Martin, H.; Pappalardo, R. R.; Ortega-Blake, I.; Marcos, E. S. *J. Chem. Phys.* **2000**, *112*, 2339.
- (145) Rick, S. W.; Stuart, S. J. *Rev. Comput. Chem.* **2002**, *18*, 89.
- (146) Lamoureux, G.; MacKerell, A. D.; Roux, B. *J. Chem. Phys.* **2003**, *119*, 5185.
- (147) Ponder, J. W.; Case, D. A. *Adv. Protein Chem.* **2003**, *66*, 27.
- (148) Kaminski, G. A.; Stern, H. A.; Berne, B. J.; Friesner, R. A. *J. Phys. Chem. A* **2004**, *108*, 621.
- (149) Patel, S.; Brooks, C. L., III. *J. Comput. Chem.* **2004**, *25*, 1.
- (150) Patel, S.; Mackerell, A. D., Jr.; Brooks, C. L., III. *J. Comput. Chem.* **2004**, *25*, 1504.
- (151) Mortier, W. J.; Van Genechten, K.; Gasteiger, J. *J. Am. Chem. Soc.* **1985**, *107*, 829.
- (152) Mortier, W. J.; Ghosh, S. K.; Shankar, S. *J. Am. Chem. Soc.* **1986**, *108*, 4315.
- (153) Rappé, A. K.; Goddard, W. A. *J. Phys. Chem.* **1991**, *95*, 3358.
- (154) Bultinck, P.; Langenaeker, W.; Lahorte, P.; De Proft, F.; Geerings, P.; Waroquier, M.; Tollenaere, J. P. *J. Phys. Chem. A* **2002**, *106*, 7887.
- (155) York, D. M.; Yang, W. *J. Chem. Phys.* **1996**, *104*, 159.
- (156) Itskowitz, P.; Berkowitz, M. L. *J. Phys. Chem. A* **1997**, *101*, 5687.
- (157) Yang, Z.-Z.; Wang, C.-S. *J. Phys. Chem. A* **1997**, *101*, 6315.
- (158) Applequist, J.; Carl, J. R.; Fung, K.-K. *J. Am. Chem. Soc.* **1972**, *94*, 2952.
- (159) Thole, B. T. *Chem. Phys.* **1981**, *59*, 341.
- (160) Stone, A. J. *Mol. Phys.* **1985**, *56*, 1065.
- (161) Winn, P. J.; Ferenczy, G. G.; Reynolds, C. A. *J. Comput. Chem.* **1999**, *20*, 704.
- (162) Rinaldi, D.; Rivail, J. L. *Theor. Chim. Acta* **1973**, *32*, 57.
- (163) Tapia, O.; Goscinski, O. *Mol. Phys.* **1975**, *29*, 1653.
- (164) Cramer, C. J.; Truhlar, D. G. Continuum solvation models. In *Solvents Effects and Chemical Reactivity*; Tapia, O., Bertran, J., Eds.; Kluwer: Dordrecht, 1996; p 1.
- (165) Ferenczy, G. G.; Reynolds, C. A. *J. Phys. Chem. A* **2001**, *105*, 11470.
- (166) French, S. A.; Sokol, A. A.; Bromley, S. T.; Catlow, C. R. A.; Rogers, S. C.; King, F.; Sherwood, P. *Angew. Chem.* **2001**, *113*, 4569.
- (167) Khaliullin, R. Z.; Bell, A. T.; Kazansky, V. B. *J. Phys. Chem. A* **2001**, *105*, 10454.
- (168) Herschend, B.; Baudin, M.; Hermansson, K. *J. Chem. Phys.* **2004**, *120*, 4939.
- (169) Bludsky, O.; Silhan, M.; Nachtigall, P.; Bucko, T.; Benco, L.; Hafner, J. *J. Phys. Chem. B* **2005**, *109*, 9631.
- (170) Monard, G.; Loos, M.; Thery, V.; Baka, K.; Rivail, J.-L. *Int. J. Quantum Chem.* **1996**, *58*, 153.
- (171) de Vries, A. H.; Sherwood, P.; Collins, S. J.; Rigby, A. M.; Rigutto, M.; Kramer, G. J. *J. Phys. Chem. B* **1999**, *103*, 6133.
- (172) Klopman, G. *J. Am. Chem. Soc.* **1964**, *86*, 4550.
- (173) Ohno, K. *Theor. Chim. Acta* **1964**, *2*, 219.
- (174) Dewar, M. J. S.; Zoebisch, E. G.; Healy, E. F.; Stewart, J. J. P. *J. Am. Chem. Soc.* **1985**, *107*, 3902.
- (175) Dewar, M. J. S.; Thiel, W. *J. Am. Chem. Soc.* **1977**, *99*, 4899.
- (176) Allinger, N. L.; Yuh, Y. H.; Lii, J. H. *J. Am. Chem. Soc.* **1989**, *111*, 8551.
- (177) Lii, J. H.; Allinger, N. L. *J. Am. Chem. Soc.* **1989**, *111*, 8566.
- (178) Lii, J. H.; Allinger, N. L. *J. Am. Chem. Soc.* **1989**, *111*, 8576.
- (179) Ponder, J. W. *TINKER, Version 4.2 ed.*; Washington University: St. Louis, MO, 2004.
- (180) Lin, H.; Zhang, Y.; Truhlar, D. G. *QMMM, Version 1.3 ed.*; University of Minnesota: Minneapolis, 2007.
- (181) Roothaan, C. C. J. *Rev. Mod. Phys.* **1951**, *23*, 69.
- (182) Easton, R. E.; Giesen, D. J.; Welch, A.; Cramer, C. J.; Truhlar, D. G. *Theor. Chem. Acc.* **1996**, *93*, 281.
- (183) Ditchfield, R.; Hehre, W. J.; Pople, J. A. *J. Chem. Phys.* **1971**, *54*, 724.
- (184) Clark, T.; Chandrasekhar, J.; Spitznagel, G. W.; Schleyer, P. v. R. *J. Comput. Chem.* **1983**, *4*, 294.
- (185) Frisch, M. J.; Pople, J. A.; Binkley, J. S. *J. Chem. Phys.* **1984**, *80*, 3265.
- (186) Rassolov, V. A.; Ratner, M. A.; Pople, J. A.; Redfern, P. C.; Curtiss, L. A. *J. Comput. Chem.* **2001**, *22*, 976.
- (187) Lee, C.; Yang, W.; Parr, R. G. *Phys. Rev. B: Condens. Matter* **1988**, *37*, 785.
- (188) Becke, A. D. *J. Chem. Phys.* **1993**, *98*, 5648.
- (189) Møller, C. M. S.; Plesset, M. S. *Phys. Rev.* **1934**, *46*, 618.
- (190) Singh, U. C.; Kollman, P. A. *J. Comput. Chem.* **1984**, *5*, 129.
- (191) Besler, B. H.; Merz, K. M., Jr.; Kollman, P. A. *J. Comput. Chem.* **1990**, *11*, 431.
- (192) Siepmann, J. I. *Adv. Chem. Phys.* **1999**, *105*, 1.
- (193) Gogonea, V.; Merz, K. M., Jr. *J. Chem. Phys.* **2000**, *112*, 3227.
- (194) Gogonea, V.; Merz, K. M., Jr. *J. Phys. Chem. B* **2000**, *104*, 2117.
- (195) Dewar, M. J. S.; Hashmall, J. A.; Venier, C. G. *J. Am. Chem. Soc.* **1968**, *90*, 1953.

- (196) Dewar, M. J. S.; Trinajstić, N. *J. Chem. Soc., Chem. Commun.* **1970**, 646.
- (197) Tavernelli, I.; Vuilleumier, R.; Sprik, M. *Phys. Rev. Lett.* **2002**, 88, 213002.
- (198) Car, R.; Parrinello, M. *Phys. Rev. Lett.* **1985**, 55, 2471.
- (199) Jaque, P.; Marenich, A.; Cramer, C. J.; Truhlar, D. G. *J. Phys. Chem. C* **2007**, asap article: 10.1021/jp066765w; Web released on 28 Mar. 2007.

CT7000107